

NASA MEMO 1-7-59L

90-4

*11-02*  
*394476*

# NASA

## MEMORANDUM

A WIND-TUNNEL INVESTIGATION OF ROTOR BEHAVIOR UNDER  
EXTREME OPERATING CONDITIONS WITH A DESCRIPTION  
OF BLADE OSCILLATIONS ATTRIBUTED  
TO PITCH-LAG COUPLING

By John W. McKee and Rodger L. Naeseth

Langley Research Center  
Langley Field, Va.

### NATIONAL AERONAUTICS AND SPACE ADMINISTRATION

WASHINGTON  
January 1959

BUSINESS, SCIENCE  
& TECHNOLOGY DEPT.

FEB 17 1959



NATIONAL AERONAUTICS AND SPACE ADMINISTRATION

---

MEMORANDUM 1-7-59L

---

A WIND-TUNNEL INVESTIGATION OF ROTOR BEHAVIOR UNDER  
EXTREME OPERATING CONDITIONS WITH A DESCRIPTION  
OF BLADE OSCILLATIONS ATTRIBUTED  
TO PITCH-LAG COUPLING

By John W. McKee and Rodger L. Naeseth

SUMMARY

A wind-tunnel investigation was made to study the behavior of a model helicopter rotor under extreme operating conditions. A 1/8-scale model of the front rotor of a tandem helicopter was built and tested to obtain blade motion and rotor aerodynamic characteristics for conditions that could be encountered in high-speed pullout maneuvers. The data are presented without analysis. A description is given in an appendix of blade oscillations that were experienced during the course of the investigation and of the part that blade pitch-lag coupling played in contributing to the oscillatory condition.

INTRODUCTION

Helicopter-rotor characteristics can be readily obtained from theoretically derived charts such as those presented in references 1 and 2 for forward flight conditions that do not result in appreciable amounts of retreating-blade stall. For some flight conditions, particularly for transient conditions such as those encountered in high-speed pullout maneuvers, extensive regions of blade stall can exist in the rotor disk. At the same time, knowledge of such factors of rotor behavior as the greatest flapping angles that will be obtained can become quite important if there is any question of interference of the rotor disk with other helicopter components. Most conventional rotor theories are not applicable under these conditions and a numerical step-by-step method of solving equations expressing the rotor behavior, as developed in references 3 and 4, must be used.

Interest in the effect of stall of the retreating blade on rotor characteristics led to an investigation for the purpose of determining the behavior that might be expected of the front rotor of a tandem

helicopter during a pullout maneuver. A  $1/8$ -scale model of the front rotor was built and tested in the Langley 300-MPH 7- by 10-foot tunnel for conditions existing in pullout maneuvers. The blade weight and stiffness were scaled to provide dynamic similarity. The model was instrumented to obtain both rotor aerodynamic and blade-motion data. The model was supported in the tunnel at several fixed angles of attack. Tests were made for a range of fixed control settings and for control pulses. The tip-speed ratio was approximately 0.30. In order to provide data in a form convenient for determining design criteria, the results of the investigation are presented in tabular form with no analysis.

During the course of the investigation, rotor-blade oscillations (predominantly lag motion) were experienced for certain operating conditions. These oscillations are discussed in the appendix. A motion-picture film supplement showing these lag oscillations has been prepared and is available on loan. A request card form and a description of the film will be found at the back of this paper, on the page immediately preceding the abstract and index cards.

#### SYMBOLS

The rotor aerodynamic coefficients are referred to axes having their origin at the point where the rotor shaft axis passes through the plane of the blade flapping hinges.

$a_{0,s}$	constant term in approximation of $\beta_s$ ; the rotor coning angle, deg
$a_{n,s}$	coefficient of $\cos n\psi$ in approximation of $\beta_s$ (positive $a_{1,s}$ is rearward tilt of rotor disk in degrees)
$\bar{A}_{0,s}$	nominal collective pitch (blade pitch at 0.75 radius with zero flapping and lag angle), deg
$\Delta\bar{A}_{0,s}$	increment in nominal collective-pitch control, deg
$A_{0,s}$	constant term in approximation of $\theta_s$ ; mean blade-pitch angle, deg
$\bar{A}_{1,s}$	nominal lateral cyclic control, positive to the right (zero flapping and lag angle), deg

$A_{n,s}$	coefficient of $\cos n\psi$ in approximation of $\theta_s$ (positive $A_{1,s}$ is feathering motion that causes rotor disk to tilt to right), deg
$b_{n,s}$	coefficient of $\sin n\psi$ in approximation of $\beta_s$ (positive $b_{1,s}$ is tilt to right of rotor disk in degrees)
$\bar{B}_{1,s}$	nominal longitudinal cyclic control, positive forward (zero flapping and lag angle), deg
$\Delta\bar{B}_{1,s}$	increment in nominal longitudinal cyclic control, deg
$B_{n,s}$	coefficient of $\sin n\psi$ in approximation of $\theta_s$ (positive $B_{1,s}$ is feathering motion that causes rotor disk to tilt forward), deg
$C_D$	drag coefficient, $\frac{D}{\frac{1}{2} \rho V^2 \pi R^2}$
$C_L$	lift coefficient, $\frac{L}{\frac{1}{2} \rho V^2 \pi R^2}$
$C_l$	rolling-moment coefficient, $\frac{M_x}{\frac{1}{2} \rho V^2 \pi R^2 R}$
$C_m$	pitching-moment coefficient, $\frac{M_y}{\frac{1}{2} \rho V^2 \pi R^2 R}$
$C_Q$	rotor-shaft torque coefficient, $\frac{Q}{\pi R^2 \rho (\Omega R)^2 R}$
$C_T$	thrust coefficient, $\frac{T}{\pi R^2 \rho (\Omega R)^2}$
$C_Y$	lateral-force coefficient, $\frac{Y}{\frac{1}{2} \rho V^2 \pi R^2}$
$D$	drag, lb

E	Young's modulus of elasticity, lb/sq in.
$E_0$	constant term in approximation of $\zeta$ ; the mean lag angle, deg
$E_n$	coefficient of $\cos n\psi$ in approximation of $\zeta$
$F_n$	coefficient of $\sin n\psi$ in approximation of $\zeta$
G	shear modulus of elasticity, lb/sq in.
I	moment of inertia in bending, in. <sup>4</sup>
J	torsional stiffness constant, in. <sup>4</sup>
L	lift, lb
$M_X$	rolling moment, lb-ft
$M_Y$	pitching moment, lb-ft
n	integer
Q	rotor-shaft torque, lb-ft
r	radius to a blade element
R	radius to blade tip, ft
T	rotor thrust, lb
t	average time of revolution, sec
$t_i$	number of rotor revolutions for control to move from initial to displaced position
V	free-stream velocity, ft/sec
Y	lateral force, lb
$\alpha$	rotor angle of attack; angle between axis of no feathering (that is, axis about which there is no pitch change) and plane perpendicular to flight path, positive when axis is inclined rearward, deg
$\alpha_s$	rotor shaft angle of attack; angle between rotor shaft and a plane perpendicular to flight path, positive when axis is inclined rearward, deg

- $\beta_s$  blade flapping angle measured at flapping hinge with respect to plane perpendicular to shaft axis, positive upwards, deg; approximated by following expression:
- $$\beta_s = a_{0,s} - a_{1,s} \cos \psi - b_{1,s} \sin \psi - a_{2,s} \cos 2\psi - b_{2,s} \sin 2\psi$$
- $\psi$  approximate blade-azimuth angle measured from downwind position in direction of rotation (as determined from shaft rotation for assumed zero lag angle), deg
- $\theta_s$  blade pitch angle at 0.75R with respect to plane perpendicular to shaft axis, deg; determined from measurements at the pitch bearing and to be more accurate should have been increased by  $\Delta\theta \approx -\frac{\beta_s \zeta}{57.3}$ ;  $\theta_s$  approximated by
- $$\theta_s = A_{0,s} - A_{1,s} \cos \psi - B_{1,s} \sin \psi - A_{2,s} \cos 2\psi - B_{2,s} \sin 2\psi$$
- $\rho$  mass density of air, slugs/cu ft
- $\zeta$  blade lag angle with respect to line perpendicular to flapping hinge, positive in direction of rotation, deg; approximated by following expression:
- $$\zeta = E_0 + E_1 \cos \psi + F_1 \sin \psi + E_2 \cos 2\psi + F_2 \sin 2\psi$$
- $\Omega$  rotor angular velocity, radians/sec

## APPARATUS

### General Model Simulation

A model, shown in figure 1, of the three-blade front rotor of a tandem-rotor helicopter was built and tested in the Langley 300-MPH 7-by 10-foot tunnel. The rotor was tested with a simple fairing enclosing the swash-plate mechanism and with a fuselage. The model was 1/8-scale and was held at fixed attitudes in the tunnel. The general arrangement of the full-scale helicopter is shown in figure 2 and some properties are listed in table I.

Dynamic similarity between the model and full-scale rotor of blade deflections and frequencies in terms of chord lengths of travel was obtained by scaling the blade weight and stiffness (from 0.197R to the tip) and the test speed. The following scaling parameters relate the

1/8-scale model to the full-scale rotor if the air density for the full-scale rotor is the same as the average model test air density of 0.00227 slug per cubic foot:

Linear dimensions . . . . .	$1/8 \times$ full scale
Area . . . . .	$(1/8)^2 \times$ full scale
Weight . . . . .	$(1/8)^3 \times$ full scale
Weight per unit length . . . . .	$(1/8)^2 \times$ full scale
Stiffness (EI and GJ) . . . . .	$(1/8)^5 \times$ full scale
Mass moment of inertia . . . . .	$(1/8)^5 \times$ full scale
Mass moment of inertia per unit length . . . . .	$(1/8)^4 \times$ full scale
Linear velocity . . . . .	$(1/8)^{0.5} \times$ full scale
Angular velocity . . . . .	$(8)^{0.5} \times$ full scale
Time . . . . .	$(1/8)^{0.5} \times$ full scale
Frequency . . . . .	$(8)^{0.5} \times$ full scale
Linear acceleration . . . . .	$1 \times$ full scale
Angular acceleration . . . . .	$8 \times$ full scale
Torque or moment . . . . .	$(1/8)^4 \times$ full scale
Power . . . . .	$(1/8)^{3.5} \times$ full scale
Reynolds number . . . . .	$(1/8)^{1.5} \times$ full scale
Mach number . . . . .	$(1/8)^{0.5} \times$ full scale
Mass constant of blade . . . . .	$1 \times$ full scale

The weight and rigidity of model parts inboard of 0.197R and in the hub and swash plate were probably greater than the scaled values.

#### Rotor Blades

Full-scale blades.- As shown in figures 2 and 3 the full-scale rotor has a radius of 264 inches and the blade proper begins at 52 inches (0.197R) from the center of rotation. The blade has a modified NACA 0019 airfoil at the 52-inch station and tapers linearly in thickness to an NACA 0015 airfoil at the 92-inch station and to an NACA 0012 airfoil at the 263-inch station, with a tip of revolution extending to the 264-inch station. The chord at station 52 is shortened to 9.32 inches by fairing the trailing edge to an approximately elliptical shape. The chord length increases linearly up to 16.5 inches at the 72-inch station and is constant at 16.5 inches from this station to the tip. The blade has a linear twist of  $7^\circ$  between the center of rotation and the tip (pitch decreasing from center to tip).

The weight and stiffness characteristics of the full-scale rotor blades are given in figure 4. The characteristics identified as "true values" are calculated values furnished by the manufacturer except in the instance of torsional stiffness which was obtained from measurements of the deflection under torque of a blade. Also shown in figure 4 are the blade properties as averaged over each of 13 finite increments of length, which were used in the design of the model blades. The weight and center of gravity of these 13 sections were in reasonable agreement with values obtained by cutting and weighing an actual blade.

Model blades.- The model rotor blades were formed by foaming plastic onto a magnesium spar in a female mold. An extra blade was cut into 13 spanwise segments to find the correction for each segment which would provide the desired weight and center of gravity. The corrections to the blades were made by cutting "lightening" holes in the foam (covered with doped paper) and by cementing ballast weights in the foam (predominantly in the nose ahead of the spar). A foam blade with no spar was also made and tested, and the foam was found to contribute about 8 percent of the total required flapwise and chordwise bending stiffness EI and 20 percent of the torsional stiffness GJ. The spar was designed to contribute the rest of the stiffness. Some sample spar test specimens were used to obtain design information. The final spar test design is shown in figure 5. The degree of attainment of the desired stiffness properties of the completed blades was checked by comparing the calculated and measured deflections resulting at several stations from application of torsion at the tip and application of normal and chord forces on a temporary spar extension 10 inches (80 inches full-scale) outboard of the tip with the root rigidly clamped. The measured deflections were smaller than desired and over the length of the blade were approximately 60 percent of the calculated chordwise deflection and 85 percent of the calculated flapwise and torsional deflection. This mismatch was greater than expected and was attributed to the contribution to the blade stiffness of the ballast weights and paper covering which had not been considered in the model design. Although the ballast weights were short (1/4 to 1/2 inch) segments of metal (steel, brass, and tungsten), a nearly continuous strip of them securely cemented in a groove in the foam just ahead of the spar was required to obtain proper weight and balance. Of the total blade weight, approximately 28 percent was ballast, 39 percent was spar, and 33 percent was foam and paper covering. The model blade weight was 70.62 grams, which represents a full-scale weight of 79.65 pounds and compares favorably with the values obtained by integration of the weight curve of figure 4 and by actually weighting a blade, 77.36 pounds and 81.04 pounds, respectively. The blade weight listed in table I includes some material between the 32- and 52-inch stations. The chordwise and spanwise location of the center of gravity of the model blades also agreed closely with the full-scale locations. Some repairs to the covering of the lightening holes in the foam were required during the course of the test program.

The cumulative effect of these repairs did not exceed a weight increase of 3 percent and the corresponding effect on the blade center of gravity was small but unknown.

The three blades were formed in the same mold and were the same size but no attempt was made to determine by measurement whether the exact twist specified was obtained or whether the three blades had identical twist. No blade trailing-edge tabs were used and one setting of the individual blade pitch links provided tracking of acceptable accuracy for the complete test program.

The natural frequencies of the nonrotating blades were determined with the blades installed on the rotor hub. Light elastic restraint at node points was used to support the blade with freedom at the flap and lag hinges and a variable-frequency air jet pulser was used to excite the blade motion. The model and full-scale frequencies are presented in table II. The excess stiffness of the model blades is seen to be reflected in frequencies slightly higher than the desired values.

#### Rotor Hub and Swash-Plate Details

The geometric arrangement of the model rotor hub and swash plate is shown in figure 6. The swash-plate gimbal pivots, lower ends of the blade-pitch links, and longitudinal control-link attachment to the swash plate are in a common plane. The lateral swash-plate cyclic-control-link attachment is below this plane. The cyclic-control-link attachment points on the lower or nonrotating swash plate were displaced from their true scale positions but lay on radial lines passing through the gimbal center and the true position; this change does not distort the hub kinematic properties.

In addition to the control provided by swash-plate position, the blade-pitch angle is dependent upon flapping and lag angles. It can be seen, for example, that if the blade is moved rearward from the position shown in figure 6 to a negative lag angle, the pitch link will rotate about its lower end, and the upper end, moving on an arc, must move down somewhat so that blade pitch is reduced. The swash-plate position shown in figure 6 corresponds to zero cyclic control and a pitch at 0.75R of  $8^{\circ} 28'$  when flapping and lag angles are zero or a pitch of  $8^{\circ}$  when the flapping angle is  $6^{\circ} 21'$  and the lag angle is  $-1^{\circ} 46'$  (back).

The hub parts and the swash plate were designed to be rugged and rigid with low friction and minimum play in the numerous moving joints. Electric motors and an air-actuated pulse device were installed for remote control of the swash-plate position through suitable linkage.

Stop settings of the flapping hinge on the model were  $30^\circ$  up and  $8^\circ$  down. The down-stop setting was greater than the full-scale value of  $4\frac{1}{2}^\circ$  to minimize stop pounding for some of the extreme operating conditions. Lag-stop settings of the model matched the full-scale values of  $10^\circ$  forward and  $20^\circ$  rearward.

Lag dampers, damper B of reference 5, were used on the model. The requirements that fluid leakage be minimized and that desired damping be maintained were met by this damper, which had no seals subject to high pressure, a small fluid reservoir, and refill ports with check valves (not shown in ref. 5) to eliminate air or vacuum bubbles.

The dampers were adjusted to simulate the viscous damping labeled "normal" or "twice normal" in figure 7, dependent upon the oil used. Because the model damper characteristics were different from those of the full-scale dampers, neither adjustment gave an exact simulation of the damping provided on the full-scale helicopter. The curve labeled "normal" represents a damping constant of 610 foot-pounds per radian per second. A piston velocity of 5 inches per second (where the curves labeled "normal" and "full-scale" intersect) is the maximum velocity occurring in a  $\pm 2^\circ$  lag oscillation at rotor rotational frequency.

#### Rotor Support and Drive

For measurement of rotor loads, the rotor was attached to a 6-component electrical strain-gage balance that was attached to the top of a support strut. The support strut was pivoted below the tunnel floor and could be locked at fixed angles to provide the desired angles of attack of the rotor. Three oil-filled dashpots were mounted at the top of the support strut to damp motions of the rotor and protect the balance from excessive deflection at resonant conditions where vibration might be encountered. Two braces from the tunnel floor to the top of the mounting strut were used to provide greater rigidity.

The rotor drive shaft was just ahead of the rotor support strut. The lower end of the drive shaft was connected by a universal joint to a two-arm air-jet reaction pinwheel type of drive device below the tunnel floor that was supplied with high pressure air. The drive device and drive shaft moved as a unit with the support strut when the angle of attack was changed. The upper end of the drive shaft drove the rotor shaft through a joint that transmitted only torque and did not have restraints that would affect the rotor loads as measured by the balance. An electrical strain gage in the drive shaft measured the drive torque.

### Fuselage and Hub Fairing

The rotor swash plate and load-measuring balance were enclosed and shielded from wind loads by either a simple fairing or a fuselage as shown in figure 1. These were attached to the support strut below the balance. The fuselage was scaled to simulate the shape of the full-scale fuselage except that an oversize fairing was required in the vicinity of the swash plate, and the tail of the fuselage was refaired to eliminate the bulge required for a rear rotor mechanism. The fuselage was built as a shell divided into eight segments attached to a central spar. Part of the top surface of the fuselage shell in the area that could possibly be struck by a blade was replaced by a paper covering.

### Instrumentation

The model was instrumented to obtain rotor aerodynamic characteristics, swash-plate control input settings, and blade-motion characteristics. Suitable electrical sensing devices at the rotor were wired to the indicating and recording equipment at the control station.

Rotor aerodynamic loads were obtained by means of the 6-component electrical strain-gage balance that connected the rotor to the mounting strut and the electrical strain-gage torque unit in the rotor drive shaft. The rotor load measurements were read from indicating instruments. They were also recorded, except shaft torque, on a multichannel recorder along with other rotor information. The recorded values were used only in preliminary tests that were made to obtain satisfactory blade tracking and balance of the rotating parts. The dynamic characteristics (frequency and damping) and low static sensitivity of the system resulted in recorded loads data that were suitable for only qualitative purposes.

Information on swash-plate position (collective, longitudinal cyclic, and lateral cyclic pitch) was obtained from flexible strain-gage beams that were deflected by movement of the motor-actuated linkage to the swash plate. These gages were calibrated with the rotor blades at zero flapping and lag angle. The control settings are referred to as nominal values since the blade-pitch angle varied with flapping and lag angle.

Blade-motion information was obtained by recording the output of three inductance-type pickups that were mounted on the rotor to sense angular position at the flapping, lag, and pitch bearings. Because of space limitations the pickups were not all mounted on one blade. The blade having the lag pickup led the blade having the flapping and pitch pickups by  $120^\circ$ . At times when the flapping angle reached  $-8^\circ$  (the

hinge down-stop setting), the position of the blade tip at zero azimuth angle was observed as it passed a graduated mast and an equivalent flapping angle was determined. For the purpose of determining the lowest position of the blade tip for transient conditions, the graduated mast was replaced by a balsa comb with teeth, pointing toward the center of rotation, that would be struck and knocked off. The azimuth reference was provided by recording the signal from a switch that was closed momentarily once each revolution by a part of the rotor drive mechanism. This switch contact occurred when the hub attachment of the blade that was instrumented for flapping and pitch angles was at zero azimuth. It should be noted that the blade-pitch-indicator measurements were in terms of angular change about the pitch axis (outboard of the flapping and lag hinges). A correction to the pitch-indicator readings to obtain blade-pitch angles is discussed in the next section.

Wires from sensing devices on rotating parts of the apparatus passed through the hollow drive shaft to a slipring unit at the lower end of the rotor drive. The rotor rotational speed was determined from an instrument that indicated the frequency of the voltage fluctuation of a multipole generator coupled to the drive shaft.

## TEST PROCEDURE AND PRESENTATION OF RESULTS

### General

The tests were made with the apparatus mounted so that the rotor was approximately centered in the test section of the Langley 300-MPH 7- by 10-foot tunnel. Preliminary tests were made to obtain satisfactory rotor tracking and balance of the rotating parts. Satisfactory tracking was achieved by making small adjustments to the pitch of the individual blades by changing the length of the pitch links which connected the blade pitch arms to the swash plate. Satisfactory balance was obtained by a trial and error process of adding weights to a small metal disk on legs attached to the top of the rotor hub. The balance weights were required to compensate for the weight of the blade-motion pickups and the swash-plate "scissors." The tracking and balance of the rotor required no further adjustments during the test program.

Complete calibrations of the instrumentation were made before the tests were started, and brief check calibrations of the blade control and motion instrumentation were made each day during the tests.

The kinematic properties of the rotor and the location and installation of the blade-motion pickups introduce certain complexities in the presentation of the data. The accuracy of the measurement of blade flapping angle was influenced by the effect of play in the flapping, the

lag, and particularly the pitch bearings, all of which were needle bearings fitted as closely as seemed practical. The effect of this play caused a total error of about  $1^\circ$ . Because of the likelihood that the blade centrifugal force will have the effect of centering all joints and minimizing the influence of this free play, the records were interpreted and presented as though this were true. Another effect of bearing play showed up in the blade pitch measurements. These undesirable hinge freedoms introduced very little error in the measurements from the pickup that measured blade pitch at the pitch bearing but a change from a nose-up to a nose-down moment on the blade would shift the calibration of the position indicators measuring control input to the swash plate by about  $1.3^\circ$ . The control inputs are presented as nominal values for the conditions of a nose-down moment on the blade and zero flapping and lag angles. When the flapping and lag angles are other than zero, changes in pitch from the nominal control inputs are produced. The pitch-pickup readings, and hence all tabular values based on them, ideally should be corrected for errors introduced by the effect of the flapping and lag angles. This correction arises because the blade axle, which was the reference point for the pitch indicator, had an effective pitch change when both flapping and lag were not zero. An approximate correction for this effect would add an increment  $\Delta\theta$  to the measured pitch angle of approximately  $-\frac{\beta_s \zeta}{57.3}$ . A kinematic effect which was sensed by the blade-pitch pickup but not by the control-input indicators is the change of blade pitch that is introduced when a change of flapping or lag angle causes the pitch link to swing about its lower or swash-plate end. Examples of the change of blade pitch for a nominal pitch of  $8.5^\circ$  (the value at zero flapping and lag) with lag angle for three flapping angles are shown in figure 8. Nominal pitch does not change, as it is determined from control input to the swash plate, the actual pitch shows a marked decrease for large negative angles of lag, and the pitch change measured by the blade-pitch pickup differs from the actual pitch by approximately  $-\frac{\beta_s \zeta}{57.3}$ . Somewhat similar curves would exist for each value of nominal pitch, and curves could also be obtained for constant values of lag angle with flapping angle as the variable.

The blade-motion records were reduced by using values read for each  $30^\circ$  of azimuth of a revolution for a 12-point harmonic analysis. No correction was added to the tabular data, but the magnitude of the error present in the blade-pitch data was evaluated in two ways in two examples: (1) by adding the increment determined for the average flapping and lag angle  $\left(-\frac{a_{0,s} E_0}{57.3}\right)$  to  $A_{0,s}$  (the constant term in the approximation of  $\theta_s$ ) and (2) by applying the appropriate correction for  $\theta_s$  to each of the 12 values used in the harmonic analysis of a cycle. The results are presented in table III. If the average correction is applied to  $A_{0,s}$ , the result is in good agreement with the values

of  $A_{0,s}$  obtained by using the correction to each of the 12 points of the harmonic analysis. The other blade-pitch terms as presented are also shown to be changed if the correction is applied to the pitch record when analyzed. The term that is probably of second greatest interest (if  $A_{0,s}$  is first) is  $B_{1,s}$  and the effect on this term is not excessively large. Records with a shaft angle of attack of  $12^\circ$  were chosen in these examples as having the greatest cyclic variation of flapping and lag angle and therefore the most pronounced distortion.

#### Tests at Zero Forward Speed

One test was made with zero wind speed in the tunnel with the swash-plate mechanism fairing and without the fuselage. Data were obtained for a range of nominal collective pitch settings with zero cyclic control and zero shaft angle of attack. The results are presented in table IV. The tunnel boundaries introduced flow distortions which would have unknown effects on the rotor characteristics.

#### Fixed-Control Tests With Tip-Speed Ratio of 0.3

Tests were made for ranges of control settings at shaft angles of attack of  $-6$ ,  $0$ ,  $6$ , and  $12^\circ$  at a tip-speed ratio  $\frac{V \cos \alpha}{\Omega R}$  of approximately 0.3. The tests were run at a constant rotor angular velocity of 80.0 radians per second and a constant tunnel dynamic pressure of 5.11 pounds per square foot. Corrections to the nominal tip-speed ratio for the air speed corresponding to the actual air density during the tests and for the tilt of the axis of no feathering would fall within the range of  $\pm 5$  percent. No corrections for tunnel jet boundaries have been applied to the data. Some of the data with collective or longitudinal cyclic pitch as the variable were obtained with zero lateral cyclic control and some with the lateral control required to provide approximately zero lateral inclination of the thrust vector as determined from the rotor balance readings. This did not generally result in exactly zero rolling moment or side-force coefficient because of balance interactions. The results are presented in table V. Twice normal lag damping was used in all cases except that given in table V(b), part (3), for which normal damping was used.

#### Transient Blade Motion Resulting From Control Pulse

Data were obtained following control pulses from initial steady-state conditions at normal model rotor speed (0.0785 sec/rev, tip-speed ratio  $\approx 0.3$ ). Two types of control increments were used. One was an

increase of nominal collective pitch of about  $4^\circ$  and the other was a combined  $4^\circ$  of nominal rearward (negative) cyclic pitch and  $2^\circ$  increase of collective pitch. The control increment was applied, held for several rotor revolutions, and then removed. The actual control increments associated with those nominal values should be obtained from harmonic-analyses data.

Blade-motion characteristics are presented in table VI for conditions after application of control increments and in table VII for conditions after return of the control to the original position. In general, the cycle analyzed in table VII was about the fourth cycle after return of the control. The characteristics after return of the control when rotor torque is high, particularly of the lag motion, are not always exactly representative because a lag oscillation, which is discussed in the appendix, was sometimes created and was in the process of decaying. A typical record obtained for motions tabulated in table VI(c) and VII(c) is shown in figure 9. Cycles to be analyzed, one after application of the control increment and one after the return of the control, have been divided into  $30^\circ$  increments of azimuth. Since the lag pickup was on a different blade from the pitch and flapping pickups, the azimuth positions are differentiated by the subscripts  $\zeta$  for lag,  $\beta$  for flapping, and  $\theta$  for pitch. The flapping trace is shown with a dashed fairing to pass through the equivalent flapping angle beyond the down stop as determined from the observed tip position at  $\psi = 0^\circ$ .

Figure 10 shows a part of a time history of a record from tables VI(b) and VII(b) illustrating the change of rotor speed that occurred during the pulse tests because the rotor drive torque remained constant. These data are shown because they were obtained for a relatively rapid  $4^\circ$  collective-pitch control pulse followed by a longer than average control-displaced time. After displacement of the control, flapping angles initially change rapidly and then more slowly. Flapping angles show a sudden change when the control is returned, but not to the original values, as the rotational speed is different.

#### CONCLUDING REMARKS

Results have been presented from a wind-tunnel investigation to determine the behavior of a model of the front rotor of a tandem helicopter under extreme operating conditions. Test conditions included a range of fixed control settings and control pulses for a tip-speed ratio of approximately 0.3. The data are presented in convenient tabular form

without analysis. Included is an appendix describing lag oscillations of the rotor blades encountered during the tests.

Langley Research Center,  
National Aeronautics and Space Administration,  
Langley Field, Va., September 2, 1958.

## APPENDIX

## LAG OSCILLATIONS OF ROTOR BLADES

Rotor-blade oscillations, predominantly lag motion with a frequency of about one cycle per three rotor revolutions, were experienced during tests of the model. When the lag oscillation was first noticed, it was thought to be a "ground resonance" coupling of the shaft displacement caused by support flexibility with the displaced center of gravity of the blade group; however, this oscillation differed from ground resonance in that damping or restraining the shaft motion did not have much effect on the blade motion. Motion pictures taken during the investigation illustrate the nature of the lag oscillations for the hovering condition and are available as a film supplement for this Memorandum.

## Rotor Behavior for Hovering With No Lag Dampers

With no lag dampers the rotor could be operated at low collective pitch and low forward speed, but an increase of either would lead to the condition of oscillatory lag motion. For the hovering condition, moderate values of collective pitch seemed to result in a condition of about neutral stability. Some difficulty was experienced in obtaining records of the time history of the blade motion, as the inception of the oscillation was difficult to anticipate; however, the situation was eased when it was found that the oscillation could be induced to start by generating a flow disturbance through the rotor disk. The amplitude of the lag oscillation would at first increase slowly to  $\pm 3^\circ$  in about 200 revolutions of the rotor and then would increase rapidly until limited by the stop settings of  $10^\circ$  forward and  $20^\circ$  rearward. Reduction of collective pitch by about  $4^\circ$  was necessary to stop the motion.

The lag motion of each of the three blades was approximately sinusoidal. The frequency was close to, but at times slightly higher or lower than,  $1/3$  of the shaft rotational frequency and approximated a simply determined natural blade-lag frequency. The three blades were phased in such manner that the motion of each blade was  $1/3$  of a cycle later than that of the blade ahead of it in the rotor disk. This type of motion results in a center of gravity of the blade group that, with respect to the shaft, is rotating counter to the direction of rotation at a frequency equal to  $1/3$  the rotational frequency or, with respect to the shaft support, is rotating at a frequency  $2/3$  the shaft rotational frequency in the same direction as the shaft. All natural frequencies of the rotor support observed after plucking the rotor support were well above the excitation frequency of  $2/3$  rotational frequency.

The lag motions were accompanied by smaller flapping and pitch oscillations so that, when the blade had rotated rearward about the lag hinge, the pitch and flapping angles were reduced.

In one test with no apparent change of operating conditions, a motion with a different blade phasing did develop. This test showed a pronounced tendency for the motion of the three blades to be in phase, and for this condition the shaft tachometer showed a noticeable fluctuation of rotational speed.

### Theory of Influence of Coupling on Oscillations

A theoretical analysis of oscillations in the hovering condition (ref. 6) indicates that a skewed hinge that results in a decrease of pitch as the blade lags back has a destabilizing influence on lag oscillations. Although the rotor of this analysis differed from the model rotor in many details, it would be expected that the model pitch-lag coupling, obtained from pitch-link action, would have a similar effect. In order to verify that the coupling contributed to the oscillatory condition, the pitch links were removed and the individual blades were locked in pitch at the pitch bearings. No oscillations were present for the hovering condition (with no lag dampers) which previously had resulted in oscillations, nor for the condition in which the collective pitch was increased by  $2^\circ$ .

Another study of the influence of coupling on blade-motion stability for the hovering condition has recently been made and is presented in reference 7. Lag instability was encountered during full-scale tests of a rotor on a WADC (Wright Air Development Center) tower. The rotor consisted of experimental blades and a hub of the type simulated by the model. A simplified stability criterion developed in reference 7 indicates that oscillations will be obtained in the hovering condition with a negative pitch-lag coupling and no dampers. In general, the behavior of the model with no lag dampers verifies this result. Lag oscillations were generally experienced after the collective pitch and the resultant lag had been increased to the point where conditions were such that the pitch-lag coupling had become negative, that is, the pitch decreased as the blade lagged back.

### Effect of Lag Dampers

Inasmuch as the model was being tested to study the blade flapping behavior, suppression of the lag oscillations was necessary, and this was accomplished by adding lag dampers.

The stability criterion of reference 7 indicates that with lag dampers some value of negative pitch-lag coupling will correspond to neutral stability, dependent upon certain blade properties and the damper coefficient. The kinematics of the rotor hub of reference 7 and the model hub were similar, but the blades of reference 7 were considerably lighter than the production blades from which the model blades were scaled (for instance, moment of inertia about the lag hinge was 25 percent less). Consequently the rotor of reference 7 would have larger flapping and lag angles and more negative coupling for comparable operating conditions. The blade differences and the damper characteristics simulated by "normal damping" combine to make the model more stable than the full-scale rotor of reference 7. The highest model blade pitch of the tests in the hovering condition with "normal damping" was  $14.5^\circ$  with a lag angle of  $15^\circ$  and a pitch-lag coupling of  $-0.5$ . For this condition, which required twice the normal rated power, no oscillations were obtained, and the stability criterion would indicate that the operating condition was just at the stability boundary.

#### Effect of Forward Speed

Forward speed introduced effects that made lag oscillations more likely to occur. No attempt was made to explore the lag stability boundary during the course of the investigation of blade flapping behavior, but some trends indicated by incidental encounters with the oscillatory condition were noted.

With no lag dampers forward speed was very effective in exciting the oscillatory condition, and the speed required to start the oscillations decreased with increased collective pitch. Of course, for forward-speed operation a normal one-cycle-per-revolution variation of flapping, lag, and pitch was present. The effect of forward speed might be attributed in part to the change of pitch-lag coupling of the linkage in different operating regions and to the reduction or removal of the damping effect of static friction in the bearings.

With normal lag damping no trouble was experienced at any forward speed for normal helicopter flight conditions. However, the lag oscillation, superimposed on the normal one-cycle-per-revolution motion, was obtained as the severity of the test condition was increased. Twice normal damping was necessary to provide a satisfactory upper limit to the test conditions. With lag damping present the amplitude of the lag oscillations could be readily controlled by small increments of pitch change.

More specifically, in contrast to the stable operation in the hovering test with normal damping, lag oscillations were obtained when the tip-speed ratio was 0.3 with about equal rotor lift or coning angle,

even though the damping was doubled and the average lag angle or torque was lower. As the rotor angle of attack was increased from  $-4^{\circ}$  to  $12^{\circ}$  (rearward tilt of the axis of no feathering), with twice normal damping, the collective pitch required for the onset of the oscillations decreased about  $4^{\circ}$ . At the same time rotor lift increased from 1.6 to 1.8 times the value for level flight and rotor torque decreased from 2.0 to 1.3 times scaled normal rated torque. One available comparison of normal and twice normal damping showed that with the higher damping the onset of oscillations occurred with  $3^{\circ}$  greater collective pitch and 30 percent higher rotor torque. Rotor theory that could be used to predict the effect of forward speed on these lag oscillations was not at hand. The effects of the kinematic properties of hub linkages with large cyclic variations of flapping, lag, and pitch and nonlinear effects of blade stall would have to be included in the theory and no such attempt was made.

## REFERENCES

1. Gessow, Alfred, and Tapscott, Robert J.: Charts for Estimating Performance of High-Performance Helicopters. NACA Rep. 1266, 1956.
2. Tapscott, Robert J., and Gessow, Alfred: Charts for Estimating Rotor-Blade Flapping Motion of High-Performance Helicopters. NACA TN 3616, 1956.
3. Gessow, Alfred, and Crim, Almer D.: A Method for Studying the Transient Blade-Flapping Behavior of Lifting Rotors at Extreme Operating Conditions. NACA TN 3366, 1955.
4. Gessow, Alfred: Equations and Procedures for Numerically Calculating the Aerodynamic Characteristics of Lifting Rotors. NACA TN 3747, 1956.
5. Silveira, Milton A., Maglieri, Domenic J., and Brooks, George W.: Results of an Experimental Investigation of Small Viscous Dampers. NACA TN 4257, 1958.
6. Morduchow, M., and Hinchey, F. G.: Theoretical Analysis of Oscillations in Hovering of Helicopter Blades With Inclined and Offset Flapping and Lagging Hinge Axes. NACA TN 2226, 1950.
7. Chou, Pei Chi: Pitch-Lag Instability of Helicopter Rotors. Jour. Am. Helicopter Soc., vol. 3, no. 3, July 1953, pp. 30-39.

TABLE I.- SOME PROPERTIES OF HELICOPTER

	Full scale	Model	
Gross weight, lb . . . . .	13,500	-----	
Maximum horsepower . . . . .	1,425	-----	
Rotor rotational speed, rpm . . . . .	270	764	
Rotor radius, ft . . . . .	22	2.75	
Blade chord, in. . . . .	16.5	2.06	
Blade washout, center line to tip, deg . . . . .	7	7	
Flapping hinge offset, percent R . . . . .	1.74	1.74	
Lag hinge offset, percent R . . . . .	5.27	5.27	
Blade weight, lb . . . . .	99.95	0.195	
Chordwise center of gravity, from leading edge, in. . . . .	} Excludes weight inboard of 0.121R	} 3.794	
Spanwise center of gravity, from center of rotation, in. . . . .			122.11
Mass moment of inertia about center of rotation, slug-ft <sup>2</sup> . . . . .			445
		0.0136	

TABLE II.- NATURAL FREQUENCIES OF NONROTATING BLADES

Mode	Model blade, cps	Model blade converted to full scale, cps	Full scale (furnished by manufacturer), cps	Full scale (measured), cps
First flapwise bending	10.9	3.86	3.67	3.55
Second flapwise bending	35.4	12.53	11.62	11.25
Third flapwise bending	74.9	26.50	25.00	22.9
First chordwise bending	-----	-----	14.11	14.15
First torsion	84.4	29.85	-----	24.0
Second torsion	-----	-----	-----	64.9

TABLE III.- EXAMPLES OF BLADE-PITCH DATA AS COMPUTED AND WITH ADDED CORRECTIONS

Data from table V(e)	$\alpha_s$ , deg	Nominal control input, deg			Blade pitch terms, deg										
		Collective $\bar{A}_{0,s}$	Lateral $\bar{A}_{1,s}$	Longitudinal $\bar{E}_{1,s}$	Uncorrected				With average correction	With correction to each of 12 points of harmonic analysis					
					$A_{0,s}$	$A_{1,s}$	$A_{2,s}$	$B_{1,s}$	$B_{2,s}$	$A_{0,s}$	$A_{1,s}$	$A_{2,s}$	$B_{1,s}$	$B_{2,s}$	
Part (8)	12	9.05	0	0	7.79	-1.32	0.28	0.25	-0.77	8.12	8.19	-0.51	-0.07	-0.12	-0.35
Part (4)	12	12.05	-1.85	0	9.41	-4.40	.51	.75	-1.15	10.35	10.50	-2.44	.03	.44	-.51

TABLE IV.- ROTOR CHARACTERISTICS WITH ZERO TUNNEL SPEED

[Shaft angle of attack and cyclic control input equal to zero;  
"normal" lag damping; no fuselage]

$\bar{A}_0, s,$ deg	$C_T$	$C_Q$	$A_0, s,$ deg	$a_0, s,$ deg	$E_0,$ deg
2.05	0.00086	0.000080	2.25	0.25	2.20
3.05	.00133	.000105	3.35	.70	2.00
4.05	.00177	.000132	4.35	.80	1.50
5.05	.00238	.000167	5.30	1.50	.85
6.05	.00286	.000194	5.90	1.90	.35
7.05	.00339	.000249	6.80	2.05	-.50
8.05	.00398	.000298	7.55	2.95	-1.50
9.05	.00451	.000341	8.40	3.05	-2.70
10.05	.00510	.000387	9.10	3.90	-3.80
11.05	.00561	.000433	9.65	4.40	-4.65
12.05	.00610	.000494	10.40	4.50	-6.00
13.05	.00644	.000561	11.15	5.15	-7.50
14.05	.00676	.000617	11.95	5.75	-8.65
15.05	.00738	.000692	12.70	6.15	-10.50
16.05	.00746	.000747	13.15	6.20	-11.45
17.05	.00780	.000817	13.90	6.15	-12.80
18.05	.00801	.000886	14.15	7.25	-14.90

TABLE V.- ROTOR CHARACTERISTICS AT A TIP-SPEED RATIO OF APPROXIMATELY 0.5

(a)  $\alpha_0 = -6^\circ$ ; no fuselage

Nominal control, deg			Aerodynamic characteristics							Feathering motion, deg					Flapping motion, deg					In-plane motion, deg				
$\bar{\alpha}_{0,s}$	$\bar{\alpha}_{1,s}$	$\bar{\beta}_{1,s}$	$C_L$	$C_D$	$C_M$	$C_1$	$C_2$	$C_3$	$C_4$	$A_{0,s}$	$A_{1,s}$	$A_{2,s}$	$B_{1,s}$	$B_{2,s}$	$a_{0,s}$	$a_{1,s}$	$a_{2,s}$	$b_{1,s}$	$b_{2,s}$	$E_0$	$E_1$	$E_2$	$F_1$	$F_2$
Part (1) $\bar{\beta}_{1,s} = -6^\circ$																								
0.0	-0.20	-0.0	0.1700	0.0199	0.0020	-0.0014	0.0079	0.00034	0.000091	5.97	-1.10	-0.05	-5.69	-0.54	4.30	11.55	0.14	0.48	0.87	0.24	0.49	-0.29	-1.46	0.77
7.0	-0.4	-0.0	0.1799	0.0228	0.0029	-0.0011	0.0049	0.000077	0.000120	6.70	-1.74	0.00	-5.77	-1.41	4.61	12.42	-0.22	0.59	0.96	0.29	0.54	-0.54	-1.54	0.79
9.0	-0.4	-0.0	0.1858	0.0244	0.0030	-0.0009	0.0030	0.000069	0.000119	7.27	-2.23	0.15	-5.63	-1.64	4.04	13.23	-0.42	0.49	1.16	0.24	0.59	-0.59	-1.54	0.69
9.0	-0.4	-0.0	0.188	0.025	0.0031	-0.0010	0.0031	0.000061	0.000119	8.26	-2.63	0.04	-5.52	-1.73	3.90	13.97	-0.42	0.74	1.16	0.34	0.70	-0.45	-2.04	1.0
Part (2) $\bar{\beta}_{1,s} = -4^\circ$																								
0.0	-0.20	-0.0	0.1600	0.0170	0.0017	-0.0010	0.0079	0.000091	0.000091	5.25	-1.08	-0.04	-5.80	-0.14	4.44	8.10	-0.15	0.35	0.08	1.04	0.24	-0.09	-0.79	0.53
6.0	-0.2	-0.0	0.1699	0.018	0.0022	-0.0008	0.0049	0.000077	0.000119	6.15	-1.56	0.00	-5.79	-0.14	3.90	8.61	0.01	0.16	0.4	1.01	0.24	-0.13	-1.00	0.46
7.0	-0.2	-0.0	0.1799	0.0206	0.0029	-0.0010	0.0049	0.000077	0.000119	6.98	-2.01	-0.04	-5.77	-0.28	4.48	9.64	-0.02	0.44	0.6	1.07	0.24	-0.20	-1.02	0.41
8.0	-0.2	-0.0	0.1899	0.023	0.0035	-0.0008	0.0049	0.000077	0.000119	7.71	-2.48	-0.11	-5.92	-0.46	4.01	10.01	-0.02	1.18	0.75	1.06	0.24	-0.40	-1.09	0.62
9.0	-0.2	-0.0	0.1999	0.0246	0.0039	-0.0007	0.0049	0.000077	0.000119	8.48	-2.87	-0.11	-5.71	-0.40	4.01	11.12	-0.45	0.95	0.77	1.02	0.24	-0.44	-1.23	0.64
10.0	-0.2	-0.0	0.209	0.026	0.0043	-0.0007	0.0049	0.000077	0.000119	9.25	-3.26	-0.10	-5.65	-0.39	4.44	11.60	-0.55	1.50	0.93	1.02	0.24	-0.49	-1.26	0.69
11.0	-0.2	-0.0	0.219	0.027	0.0047	-0.0007	0.0049	0.000077	0.000119	9.99	-3.63	-0.09	-5.53	-0.30	4.69	12.12	-0.64	1.28	1.19	1.02	0.24	-0.45	-2.72	0.69
Part (3) $\bar{\beta}_{1,s} = -2^\circ$																								
0.0	-0.20	-0.0	0.0999	0.0061	0.0009	-0.0007	0.0079	0.000107	0.000107	5.29	-1.01	0.00	-1.87	-0.10	2.42	5.09	-0.14	-0.01	0.47	1.04	0.12	-0.02	-0.34	0.18
6.0	-0.2	-0.0	0.1099	0.0074	0.0014	-0.0007	0.0049	0.000107	0.000107	6.15	-1.44	0.00	-1.88	-0.12	3.29	6.30	-0.07	0.16	0.11	1.05	0.17	-0.07	-0.34	0.24
7.0	-0.2	-0.0	0.1199	0.0084	0.0019	-0.0007	0.0049	0.000107	0.000107	7.02	-1.79	-0.01	-1.95	-0.13	4.06	7.53	0.00	0.48	0.6	1.07	0.17	-0.14	-0.34	0.31
8.0	-0.2	-0.0	0.1299	0.0094	0.0024	-0.0007	0.0049	0.000107	0.000107	7.75	-2.18	0.00	-1.80	-0.18	4.48	8.19	0.01	0.41	0.6	1.04	0.17	-0.14	-0.34	0.31
9.0	-0.2	-0.0	0.1399	0.0104	0.0029	-0.0007	0.0049	0.000107	0.000107	8.48	-2.57	0.00	-1.78	-0.17	4.61	8.86	-0.49	0.94	0.72	1.02	0.17	-0.14	-1.03	0.41
10.0	-0.2	-0.0	0.1499	0.0114	0.0034	-0.0007	0.0049	0.000107	0.000107	9.25	-2.94	0.00	-1.72	-0.15	4.74	9.69	-0.50	1.09	1.05	1.01	0.17	-0.14	-1.24	0.44
11.0	-0.2	-0.0	0.1599	0.0124	0.0039	-0.0007	0.0049	0.000107	0.000107	9.97	-3.24	0.00	-1.74	-0.16	4.44	10.33	-0.80	1.43	1.15	1.05	0.17	-0.14	-2.48	0.59
Part (4) $\bar{\beta}_{1,s} = 0^\circ$																								
0.0	-0.20	0.0	0.0999	0.0061	0.0009	-0.0007	0.0079	0.000104	0.000104	4.18	-0.68	0.00	-0.07	-0.02	0.90	2.66	0.07	-0.16	0.44	1.04	0.00	-0.01	-0.10	0.08
6.0	-0.2	0.0	0.1099	0.0074	0.0014	-0.0007	0.0049	0.000104	0.000104	5.02	-0.96	-0.04	-0.07	-0.02	1.94	3.14	0.13	-0.02	0.36	1.04	0.00	-0.04	-0.16	0.10
7.0	-0.2	0.0	0.1199	0.0084	0.0019	-0.0007	0.0049	0.000104	0.000104	5.98	-1.20	-0.04	-0.19	-0.11	2.43	4.06	-0.14	0.31	0.34	1.07	0.00	-0.04	-0.16	0.12
8.0	-0.2	0.0	0.1299	0.0094	0.0024	-0.0007	0.0049	0.000104	0.000104	6.85	-1.70	-0.02	-0.00	-0.02	3.00	5.00	0.00	0.40	0.51	1.09	0.00	-0.04	-0.16	0.18
9.0	-0.2	0.0	0.1399	0.0104	0.0029	-0.0007	0.0049	0.000104	0.000104	7.71	-2.21	-0.01	0.00	-0.04	4.02	6.35	0.16	0.49	0.72	1.06	0.00	-0.04	-0.16	0.24
10.0	-0.2	0.0	0.1499	0.0114	0.0034	-0.0007	0.0049	0.000104	0.000104	8.48	-2.74	0.00	0.00	-0.43	4.42	6.50	0.14	0.50	0.92	1.02	0.00	-0.14	-1.26	0.27
11.0	-0.2	0.0	0.1599	0.0124	0.0039	-0.0007	0.0049	0.000104	0.000104	9.25	-3.24	0.00	0.00	-0.46	4.82	7.44	-0.58	1.14	1.01	1.01	0.00	-0.14	-1.74	0.27
12.0	-0.2	0.0	0.1699	0.0134	0.0044	-0.0007	0.0049	0.000104	0.000104	9.99	-3.63	0.00	0.00	-0.35	4.07	8.00	-0.73	1.41	1.01	1.01	0.00	-0.14	-2.06	0.31
Part (5) $\bar{\beta}_{1,s} = 2^\circ$																								
0.0	-0.20	0.0	0.0999	0.0061	0.0009	-0.0007	0.0079	0.000112	0.000112	4.23	-0.69	0.00	1.80	-0.07	0.98	0.96	-0.04	0.44	0.53	0.90	0.07	0.00	0.00	0.04
6.0	-0.2	0.0	0.1099	0.0074	0.0014	-0.0007	0.0049	0.000112	0.000112	5.02	-0.96	0.00	1.88	-0.07	1.94	1.50	0.00	0.61	0.53	1.0	0.00	-0.04	-0.16	0.08
7.0	-0.2	0.0	0.1199	0.0084	0.0019	-0.0007	0.0049	0.000112	0.000112	5.98	-1.20	-0.04	1.79	-0.11	2.43	2.50	0.00	0.49	0.54	1.07	0.00	-0.04	-0.16	0.11
8.0	-0.2	0.0	0.1299	0.0094	0.0024	-0.0007	0.0049	0.000112	0.000112	6.85	-1.70	-0.02	1.93	-0.11	3.14	3.47	0.00	0.78	0.60	1.04	0.00	-0.04	-0.16	0.14
9.0	-0.2	0.0	0.1399	0.0104	0.0029	-0.0007	0.0049	0.000112	0.000112	7.71	-2.21	-0.01	2.00	-0.12	4.02	4.34	0.16	0.69	0.72	1.02	0.00	-0.04	-0.16	0.18
10.0	-0.2	0.0	0.1499	0.0114	0.0034	-0.0007	0.0049	0.000112	0.000112	8.48	-2.74	0.00	2.10	-0.13	4.14	5.16	0.15	1.00	0.92	1.02	0.00	-0.14	-1.09	0.14
11.0	-0.2	0.0	0.1599	0.0124	0.0039	-0.0007	0.0049	0.000112	0.000112	9.25	-3.24	0.00	2.16	-0.12	4.62	6.00	0.14	1.50	1.05	1.01	0.00	-0.14	-1.48	0.26
12.0	-0.2	0.0	0.1699	0.0134	0.0044	-0.0007	0.0049	0.000112	0.000112	10.00	-3.63	0.00	2.24	-0.11	4.90	6.83	-0.12	1.54	1.14	1.01	0.00	-0.14	-2.06	0.31
Part (6) $\bar{\beta}_{1,s} = 4^\circ$																								
0.0	-0.20	0.0	0.0500	0.0021	-0.0004	-0.0004	0.0079	0.000114	0.000114	4.73	0.22	0.03	3.79	-0.05	0.24	-1.34	0.16	0.69	0.25	1.28	0.03	0.00	-0.02	0.05
6.0	-0.2	0.0	0.0571	0.0029	-0.0007	-0.0004	0.0049	0.000114	0.000114	5.69	-0.52	0.01	3.60	-0.04	0.93	-0.80	0.03	0.69	0.46	1.45	0.03	-0.01	-0.02	0.02
7.0	-0.2	0.0	0.0640	0.0038	-0.0009	-0.0004	0.0049	0.000114	0.000114	6.67	-0.97	0.00	3.66	-0.04	1.64	-0.06	0.17	0.66	0.46	1.26	0.03	-0.01	-0.04	0.02
8.0	-0.2	0.0	0.0709	0.0046	-0.0011	-0.0004	0.0049	0.000114	0.000114	7.62	-1.50	-0.02	3.90	-0.04	2.40	1.07	0.06	0.76	0.43	1.07	0.00	-0.06	-0.24	0.07
9.0	-0.2	0.0	0.0778	0.0054	-0.0013	-0.0004	0.0049	0.000114	0.000114	8.41	-1.93	-0.03	3.90	-0.11	3.14	1.90	0.21	0.85	0.69	1.02	0.00	-0.06	-0.41	0.08
10.0	-0.2	0.0	0.0847	0.0062	-0.0015	-0.0004	0.0049	0.000114	0.000114	9.21	-2.33	-0.04	4.02	-0.18	3.84	2.89	0.25	0.91	0.80	1.01	0.00	-0.06	-0.67	0.10
11.0	-0.2	0.0	0.0916	0.0070	-0.0017	-0.0004	0.0049	0.000114	0.000114	9.97	-2.72	-0.10	4.11	-0.15	4.00	4.11	0.22	1.11	1.00	1.01	0.00	-0.14	-1.02	0.12
12.0	-0.2	0.0	0.0985	0.0078	-0.0019	-0.0004	0.0049	0.000114	0.000114	10.72	-3.12	-0.14	4.20	-0.10	4.36	5.00	0.19	1.60	1.14	1.01	0.00	-0.14	-1.49	0.14
Part (7) $\bar{\beta}_{1,s} = 6^\circ$																								
0.0	-0.20	0.0	0.0100	0.0006	-0.0001	-0.0001	0.0079	0.000099	0.000099	4.95	0.08	0.00	3.63	0.00	-0.57	-3.77	0.09	0.37	0.33	1.54	0.00	0.02	-0.07	0.12
6.0	-0.2	0.0	0.0171	0.0008	-0.0002	-0.0001	0.0049	0.000099	0.000099	5.71	-0.14	0.00	3.82	-0.10	1.41	-3.12	0.08	0.49	0.43	1.64	0.00	-0.07	-0.01	0.21
7.0	-0.2	0.0	0.0240	0.0010	-0.0003	-0.0001	0.0049	0.000099	0.000099	6.47	-0.27	0.00	3.87	-0.14	1.09	-2.51	0.05	0.53	0.60	1.20	0.00	-0.07	-0.03	0.08
8.0	-0.2	0.0	0.0309	0.0012	-0.0004	-0.0001	0.0049	0.000099	0.000099	7.21	-0.40	0.00	3.80	-0.12	1.79	-1.47	0.10	0.78	0.53	1.07	0.00	-0.07	-0.03	0.07
9.0	-0.2	0.0	0.0378	0.0014																				

TABLE V. - ROTOR CHARACTERISTICS AT A TIP-SPEED RATIO OF APPROXIMATELY 0.5 - Continued

(b)  $\alpha_g = 0^\circ$ ; no fuselage

Nominal control, deg			Aerodynamic characteristics							Feathering motion, deg					Flapping motion, deg					In-plane motion, deg							
$\bar{A}_{0,s}$	$\bar{A}_{1,s}$	$\bar{A}_{2,s}$	$C_L$	$C_D$	$C_m$	$C_{L1}$	$C_{Y1}$	$C_{Q1}$	$A_{0,s}$	$A_{1,s}$	$A_{2,s}$	$B_{1,s}$	$B_{2,s}$	$B_{3,s}$	$a_{1,s}$	$a_{2,s}$	$a_{3,s}$	$b_{1,s}$	$b_{2,s}$	$b_{3,s}$	$E_0$	$E_1$	$E_2$	$F_1$	$F_2$		
Part (1) $\bar{B}_{1,s} = -5^\circ$																											
6.0°	-0.40	4.0	0.1334	0.0304	0.0015	-0.0010	0.0023	0.000137	5.57	-1.10	0.00	-5.72	-0.51	5.18	10.11	0.51	0.34	0.69	0.46	0.44	-0.15	-1.15	0.16				
7.0°	-0.40	4.0	0.1342	0.0306	0.0015	-0.0009	0.0023	0.000137	6.39	-1.28	0.01	-5.62	-0.41	6.79	10.87	-0.06	0.19	0.12	0.46	0.44	-0.15	-1.15	0.16				
8.0°	-0.40	4.0	0.1350	0.0308	0.0015	-0.0007	0.0023	0.000137	7.21	-1.46	0.11	-5.57	-0.35	7.06	11.60	-0.10	0.00	0.00	0.46	0.44	-0.15	-1.15	0.16				
9.0°	-0.40	4.0	0.1358	0.0310	0.0015	-0.0005	0.0023	0.000137	8.03	-1.64	0.21	-5.50	-0.26	7.41	12.34	-0.16	0.10	0.05	0.46	0.44	-0.15	-1.15	0.16				
10.0°	-0.40	4.0	0.1366	0.0312	0.0015	-0.0003	0.0023	0.000137	8.85	-1.82	0.31	-5.43	-0.17	7.76	13.07	-0.22	0.20	0.10	0.46	0.44	-0.15	-1.15	0.16				
11.0°	-0.40	4.0	0.1374	0.0314	0.0015	-0.0001	0.0023	0.000137	9.67	-2.00	0.41	-5.36	-0.10	8.11	13.80	-0.28	0.30	0.15	0.46	0.44	-0.15	-1.15	0.16				
Part (2) $\bar{B}_{1,s} = 0^\circ$																											
6.0°	-0.40	0.0	0.1310	0.0300	-0.0011	-0.0004	0.0009	0.000140	5.45	-0.90	0.00	0.06	-0.17	4.59	5.15	0.24	0.69	0.79	0.55	0.50	-0.91	0.50	-0.09	-0.76	0.12		
7.0°	-0.40	0.0	0.1318	0.0302	-0.0011	-0.0003	0.0009	0.000140	6.27	-1.08	0.01	0.06	-0.10	4.78	5.44	0.24	0.69	0.79	0.55	0.50	-0.91	0.50	-0.09	-0.76	0.12		
8.0°	-0.40	0.0	0.1326	0.0304	-0.0011	-0.0002	0.0009	0.000140	7.09	-1.26	0.02	0.17	-0.03	4.97	5.69	0.24	0.69	0.79	0.55	0.50	-0.91	0.50	-0.09	-0.76	0.12		
9.0°	-0.40	0.0	0.1334	0.0306	-0.0011	-0.0001	0.0009	0.000140	7.91	-1.44	0.03	0.24	0.04	5.16	5.94	0.24	0.69	0.79	0.55	0.50	-0.91	0.50	-0.09	-0.76	0.12		
10.0°	-0.40	0.0	0.1342	0.0308	-0.0011	0.0000	0.0009	0.000140	8.73	-1.62	0.04	0.31	0.13	5.35	6.19	0.24	0.69	0.79	0.55	0.50	-0.91	0.50	-0.09	-0.76	0.12		
11.0°	-0.40	0.0	0.1350	0.0310	-0.0011	0.0001	0.0009	0.000140	9.55	-1.80	0.05	0.38	0.22	5.54	6.44	0.24	0.69	0.79	0.55	0.50	-0.91	0.50	-0.09	-0.76	0.12		
12.0°	-0.40	0.0	0.1358	0.0312	-0.0011	0.0002	0.0009	0.000140	10.37	-1.98	0.06	0.45	0.31	5.73	6.69	0.24	0.69	0.79	0.55	0.50	-0.91	0.50	-0.09	-0.76	0.12		
13.0°	-0.40	0.0	0.1366	0.0314	-0.0011	0.0003	0.0009	0.000140	11.19	-2.16	0.07	0.52	0.40	5.92	6.94	0.24	0.69	0.79	0.55	0.50	-0.91	0.50	-0.09	-0.76	0.12		
14.0°	-0.40	0.0	0.1374	0.0316	-0.0011	0.0004	0.0009	0.000140	12.01	-2.34	0.08	0.59	0.49	6.11	7.19	0.24	0.69	0.79	0.55	0.50	-0.91	0.50	-0.09	-0.76	0.12		
15.0°	-0.40	0.0	0.1382	0.0318	-0.0011	0.0005	0.0009	0.000140	12.83	-2.52	0.09	0.66	0.58	6.30	7.44	0.24	0.69	0.79	0.55	0.50	-0.91	0.50	-0.09	-0.76	0.12		
16.0°	-0.40	0.0	0.1390	0.0320	-0.0011	0.0006	0.0009	0.000140	13.65	-2.70	0.10	0.73	0.67	6.49	7.69	0.24	0.69	0.79	0.55	0.50	-0.91	0.50	-0.09	-0.76	0.12		
17.0°	-0.40	0.0	0.1398	0.0322	-0.0011	0.0007	0.0009	0.000140	14.47	-2.88	0.11	0.80	0.76	6.68	7.94	0.24	0.69	0.79	0.55	0.50	-0.91	0.50	-0.09	-0.76	0.12		
Part (3) $\bar{B}_{1,s} = 5^\circ$ ; "normal" lag damping																											
4.0°	-0.35	5.0	0.0711	0.0074	-0.0002	-0.0003	0.0011	0.000044	4.21	-0.54	0.04	2.96	-0.04	1.49	-0.05	0.02	0.58	0.44	1.55	0.17	0.00	0.04	0.01				
5.0°	-0.35	5.0	0.0719	0.0074	-0.0002	-0.0003	0.0011	0.000044	5.03	-0.68	0.09	2.96	-0.02	2.28	1.02	0.01	0.85	0.49	1.20	0.27	-0.01	-0.14	0.01				
6.0°	-0.35	5.0	0.0727	0.0074	-0.0002	-0.0003	0.0011	0.000044	5.85	-0.82	0.14	2.96	-0.01	3.10	1.79	0.08	1.45	0.46	0.56	0.28	-0.08	-0.16	0.02				
7.0°	-0.35	5.0	0.0735	0.0074	-0.0002	-0.0003	0.0011	0.000044	6.67	-0.96	0.19	2.96	-0.10	3.44	2.84	-0.33	0.61	0.60	-0.46	0.39	-0.09	-0.17	0.04				
8.0°	-0.35	5.0	0.0743	0.0074	-0.0002	-0.0003	0.0011	0.000044	7.49	-1.10	0.24	2.96	-0.20	3.90	3.53	0.00	1.37	0.64	-1.80	0.66	-0.13	-1.04	0.08				
9.0°	-0.35	5.0	0.0751	0.0074	-0.0002	-0.0003	0.0011	0.000044	8.31	-1.24	0.29	2.96	-0.30	4.47	4.26	0.10	0.92	1.01	-2.58	0.77	-0.26	-1.57	0.23				
10.0°	-0.35	5.0	0.0759	0.0074	-0.0002	-0.0003	0.0011	0.000044	9.13	-1.38	0.34	2.96	-0.40	5.04	4.95	0.20	1.01	1.01	-3.81	0.75	-0.35	-1.57	0.14				
11.0°	-0.35	5.0	0.0767	0.0074	-0.0002	-0.0003	0.0011	0.000044	9.95	-1.52	0.39	2.96	-0.50	5.61	5.67	0.30	1.05	1.05	-5.07	0.65	-0.44	-2.02	0.07				
12.0°	-0.35	5.0	0.0775	0.0074	-0.0002	-0.0003	0.0011	0.000044	10.77	-1.66	0.44	2.96	-0.60	6.18	6.33	0.40	1.07	1.01	-6.38	0.51	-0.54	-2.50	0.01				
13.0°	-0.35	5.0	0.0783	0.0074	-0.0002	-0.0003	0.0011	0.000044	11.59	-1.80	0.49	2.96	-0.70	6.76	7.02	0.50	1.02	1.02	-7.68	0.37	-0.63	-3.03	0.01				
14.0°	-0.35	5.0	0.0791	0.0074	-0.0002	-0.0003	0.0011	0.000044	12.41	-1.94	0.54	2.96	-0.80	7.34	7.68	0.60	1.02	1.02	-8.98	0.23	-0.72	-3.56	0.01				
15.0°	-0.35	5.0	0.0799	0.0074	-0.0002	-0.0003	0.0011	0.000044	13.23	-2.08	0.59	2.96	-0.90	7.92	8.34	0.70	1.02	1.02	-10.28	0.09	-0.81	-4.09	0.01				
16.0°	-0.35	5.0	0.0807	0.0074	-0.0002	-0.0003	0.0011	0.000044	14.05	-2.22	0.64	2.96	-1.00	8.50	9.00	0.80	1.02	1.02	-11.58	0.00	-0.90	-4.61	0.01				
Part (4) $\bar{B}_{1,s} = 5^\circ$ ; "twice normal" lag damping																											
4.0°	-0.35	5.0	0.1132	0.0144	0.0004	0.0001	-0.0001	0.000048	7.97	-2.26	0.03	2.85	-0.28	4.55	4.70	0.10	1.58	1.01	-3.79	0.74	-0.20	-1.54	0.05				
5.0°	-0.35	5.0	0.1140	0.0144	0.0004	0.0001	-0.0001	0.000048	8.79	-2.40	0.09	3.05	-0.21	5.12	5.54	0.20	1.46	0.99	-3.09	0.67	-0.23	-1.87	0.04				
6.0°	-0.35	5.0	0.1148	0.0144	0.0004	0.0001	-0.0001	0.000048	9.61	-2.54	0.14	3.05	-0.13	5.69	6.37	0.30	1.34	1.06	-2.20	0.61	-0.25	-2.20	0.04				
7.0°	-0.35	5.0	0.1156	0.0144	0.0004	0.0001	-0.0001	0.000048	10.43	-2.68	0.19	3.05	-0.06	6.26	7.19	0.40	1.22	1.06	-1.40	0.55	-0.27	-2.52	0.04				
8.0°	-0.35	5.0	0.1164	0.0144	0.0004	0.0001	-0.0001	0.000048	11.25	-2.82	0.24	3.05	-0.01	6.84	8.00	0.50	1.10	1.09	-0.50	0.49	-0.28	-2.84	0.04				
9.0°	-0.35	5.0	0.1172	0.0144	0.0004	0.0001	-0.0001	0.000048	12.07	-2.96	0.29	3.05	0.04	7.42	8.81	0.60	1.00	1.09	0.40	0.43	-0.29	-3.16	0.04				
10.0°	-0.35	5.0	0.1180	0.0144	0.0004	0.0001	-0.0001	0.000048	12.89	-3.10	0.34	3.05	0.09	8.00	9.62	0.70	0.89	1.09	-0.50	0.37	-0.30	-3.48	0.04				
11.0°	-0.35	5.0	0.1188	0.0144	0.0004	0.0001	-0.0001	0.000048	13.71	-3.24	0.39	3.05	0.14	8.58	10.43	0.80	0.77	1.09	-1.40	0.35	-0.31	-3.80	0.04				
12.0°	-0.35	5.0	0.1196	0.0144	0.0004	0.0001	-0.0001	0.000048	14.53	-3.38	0.44	3.05	0.19	9.16	11.24	0.90	0.65	1.09	-2.30	0.31	-0.32	-4.12	0.04				
13.0°	-0.35	5.0	0.1204	0.0144	0.0004	0.0001	-0.0001	0.000048	15.35	-3.52	0.49	3.05	0.24	9.74	12.05	1.00	0.53	1.09	-3.20	0.27	-0.33	-4.44	0.04				
14.0°	-0.35	5.0	0.1212	0.0144	0.0004	0.0001	-0.0001	0.000048	16.17	-3.66	0.54	3.05	0.29	10.32	12.86	1.10	0.41	1.09	-4.10	0.23	-0.34	-4.76	0.04				
15.0°	-0.35	5.0	0.1220	0.0144	0.0004	0.0001	-0.0001	0.000048	16.99	-3.80	0.59	3.05	0.34	10.90	13.67	1.20	0.29	1.09	-5.00	0.19	-0.35	-5.08	0.04				
16.0°	-0.35	5.0	0.1228	0.0144	0.0004	0.0001	-0.0001	0.000048	17.81	-3.94	0.64	3.05	0.39	11.48	14.48	1.30	0.17	1.09	-5.90	0.15	-0.36	-5.40	0.04				
17.0°	-0.35	5.0	0.1236	0.0144	0.0004	0.0001	-0.0001	0.000048	18.63	-4.08	0.69	3.05	0.44	12.06	15.29	1.40	0.05	1.09	-6.80	0.11	-0.37	-5.72	0.04				
Part (5) $\bar{B}_{1,s} = 4^\circ$																											
9.0°	0	4.0	0.1332	0.0107	0.0011	0.0011	0.0010	0.000068	8.44	-0.61	0.00	5.72	-0.51</														

TABLE V. - ROTOR CHARACTERISTICS AT A TIP-SPEED RATIO OF APPROXIMATELY 0.3 - Continued

(c)  $\alpha_B = 6^\circ$ ; no fuselage

Nominal Control, deg			Aerodynamic characteristics							Feathering motion, deg					Flapping motion, deg					In-plane motion, deg				
$\bar{A}_{0,s}$	$\bar{A}_{1,s}$	$\bar{B}_{1,s}$	$C_L$	$C_D$	$C_m$	$C_{l_1}$	$C_Y$	$C_Q$	$A_{0,s}$	$A_{1,s}$	$A_{2,s}$	$B_{1,s}$	$B_{2,s}$	$a_{0,s}$	$a_{1,s}$	$a_{2,s}$	$b_{1,s}$	$b_{2,s}$	$E_0$	$E_1$	$E_2$	$F_1$	$F_2$	
Part (1) $\bar{B}_{1,s} = -4^\circ$																								
6.0	-0.4	-4.0	0.1570	0.0497	0.0038	-0.0012	0.0033	0.000140	9.01	-1.22	0.00	-3.57	-0.47	6.16	11.54	0.00	0.59	1.08	0.80	0.79	-0.31	-2.66	0.77	
7.0	-0.70	-4.0	0.1636	0.0548	0.0036	-0.0010	0.0022	0.000208	9.84	-1.67	0.06	-3.94	-0.60	6.36	12.46	-0.20	1.07	1.26	-0.73	1.03	-0.48	-3.18	0.86	
8.0	-1.0	-4.0	0.1713	0.0582	0.0034	-0.0008	0.0009	0.000277	10.52	-2.11	0.17	-3.44	-0.56	6.83	12.96	-0.51	1.31	1.06	-2.09	1.26	-0.64	-3.45	0.90	
9.0	-1.3	-4.0	0.1797	0.0595	0.0033	-0.0007	0.0003	0.000345	11.14	-2.69	0.28	-3.48	-0.53	7.05	13.89	-0.69	1.39	0.82	-3.24	1.29	-0.70	-4.00	0.96	
10.0	-1.6	-4.0	0.1866	0.0610	0.0033	-0.0006	0.0000	0.000419	11.72	-3.16	0.24	-3.16	-0.51	7.24	14.84	-0.84	1.41	0.94	-4.17	1.15	-0.95	-4.53	1.11	
11.0	-1.9	-4.0	0.1938	0.0623	0.0032	-0.0005	0.0002	0.000480	12.27	-3.63	0.11	-3.02	-0.48	7.63	15.02	-1.01	1.17	1.09	-6.04	0.82	-0.83	-4.62	1.12	
Part (2) $\bar{B}_{1,s} = -5^\circ$																								
6.0	-0.6	-3.0	0.1525	0.0469	0.0027	0.0002	-0.0004	0.000134	4.80	-1.34	-0.06	-2.76	-0.31	6.46	10.40	-0.20	0.93	0.90	0.39	0.82	-0.33	-2.44	0.51	
7.0	-0.90	-3.0	0.1607	0.0487	0.0025	0.0004	-0.0015	0.000226	5.59	-1.91	-0.07	-2.57	-0.54	6.7	11.27	0.00	0.88	0.25	-0.86	0.66	-0.39	-2.93	0.73	
8.0	-1.40	-3.0	0.1697	0.0521	0.0023	0.0009	-0.002	0.000296	6.30	-2.66	0.06	-2.45	-0.63	6.99	12.06	-0.34	0.90	0.99	-1.99	0.89	-0.48	-3.29	0.71	
Part (3) $\bar{B}_{1,s} = -2^\circ$																								
5.0	-0.80	-2.0	0.1444	0.0377	0.0022	-0.0007	0.0001	0.000064	4.95	-1.29	0.05	-1.84	-0.21	4.72	8.34	-0.08	0.66	0.89	1.76	0.50	-0.18	-1.48	0.25	
6.0	-1.0	-2.0	0.1523	0.0411	0.0020	-0.0010	0.0004	0.000122	5.68	-1.59	0.02	-1.80	-0.36	5.29	9.33	-0.17	0.78	0.99	1.44	0.72	-0.22	-1.82	0.41	
7.0	-1.3	-2.0	0.1594	0.0445	0.0017	-0.0008	0.0002	0.000190	6.48	-1.84	0.14	-1.60	-0.53	5.46	10.25	-0.14	1.09	1.16	-0.99	0.82	-0.33	-2.29	0.46	
8.0	-1.6	-2.0	0.1690	0.0478	0.0017	-0.0007	0.0001	0.000267	7.12	-2.40	0.16	-1.72	-0.72	6.09	11.00	-0.55	1.08	1.21	-1.86	0.86	-0.39	-2.72	0.62	
9.0	-1.9	-2.0	0.1740	0.0512	0.0015	-0.0005	0.0003	0.000347	7.99	-2.75	0.17	-1.79	-0.70	6.08	11.78	-0.25	1.60	1.11	-3.22	1.10	-0.42	-3.05	0.69	
10.0	-2.0	-2.0	0.1807	0.048	0.0015	-0.0001	0.000421	8.71	-3.16	0.27	-1.67	-0.90	6.27	12.59	-0.55	2.04	1.14	-4.98	1.00	-0.50	-3.54	0.66		
11.0	-2.20	-2.0	0.181	0.065	0.0019	-0.0008	0.000486	9.42	-3.38	0.43	-1.72	-0.98	6.44	13.04	-0.61	2.65	1.06	-6.59	1.51	-0.75	-3.66	0.89		
12.0	-2.25	-2.0	0.1907	0.0584	0.0010	-0.0006	0.000543	9.81	-4.04	0.59	-1.48	-1.25	6.84	13.28	-0.63	2.60	1.05	-6.78	1.29	-0.72	-3.96	0.89		
13.0	-2.40	-2.0	0.1937	0.0617	0.0007	-0.0009	0.000604	10.51	-4.55	0.60	-1.10	-1.25	6.88	13.95	-1.00	2.76	1.21	-8.98	1.46	-0.80	-4.27	0.89		
14.0	-2.45	-2.0	0.1976	0.0582	0.0008	-0.0018	0.000670	11.02	-5.02	0.79	-1.20	-1.45	7.52	14.29	-1.36	3.14	1.29	-9.93	1.73	-0.90	-4.49	1.03		
Part (4) $\bar{B}_{1,s} = -1.5^\circ$																								
5.1	-0.60	-1.5	0.1499	0.0397	0.0021	0.0001	0.0005	0.000111	5.96	-0.98	0.06	-1.39	-0.31	6.25	8.15	0.10	0.75	0.86	1.27	0.67	-0.25	-1.66	0.50	
6.0	-0.90	-1.5	0.1532	0.0396	0.0028	-0.0005	0.0009	0.000161	6.65	-1.39	0.12	-1.31	-0.36	6.45	8.58	-0.14	0.85	1.06	1.46	0.68	-0.34	-1.92	0.38	
7.0	-1.05	-1.5	0.1570	0.0412	0.0036	0.0016	-0.001	0.000230	7.38	-1.86	0.04	-1.34	-0.38	6.83	9.64	-0.15	1.33	0.93	-1.14	1.04	-0.45	-2.34	0.53	
Part (5) $\bar{B}_{1,s} = 0^\circ$																								
5.0	-0.80	0.0	0.1364	0.0314	0.0010	-0.0006	0.0014	0.000072	5.05	-0.98	-0.01	-0.02	-0.20	4.67	6.00	0.35	0.46	0.89	1.73	0.47	-0.14	-1.06	0.15	
6.0	-1.10	0.0	0.1465	0.0400	-0.0012	0.0004	-0.0013	0.000135	5.69	-1.66	0.09	0.06	-0.35	5.01	7.19	0.07	0.59	0.90	1.65	0.65	-0.18	-1.44	0.20	
6.0	-1.0	0.0	0.1409	0.0345	0.0012	-0.0008	0.0011	0.000142	5.18	-1.09	0.02	0.18	-0.30	5.43	7.23	-0.16	0.83	0.98	1.46	0.59	-0.20	-1.55	0.21	
7.0	-1.00	0.0	0.1510	0.0384	0.0014	-0.0008	0.0020	0.000209	6.03	-1.66	0.10	0.18	-0.35	5.68	8.11	-0.12	1.08	0.96	-0.79	0.77	-0.31	-1.96	0.28	
8.0	-1.15	0.0	0.1581	0.039	0.0028	-0.0009	0.0024	0.000267	6.67	-2.00	0.12	-0.20	-0.27	6.23	8.84	0.17	1.29	1.11	-1.76	0.90	-0.43	-2.24	0.46	
9.0	-1.00	0.0	0.1636	0.0403	0.0030	-0.0000	0.0024	0.000341	7.47	-2.94	0.09	0.32	-0.56	6.40	9.15	0.04	1.75	1.14	-3.18	1.01	-0.35	-2.45	0.43	
10.0	-1.95	0.0	0.1708	0.038	0.0035	-0.0019	0.0025	0.000426	8.16	-3.24	-0.02	0.55	-0.67	6.75	9.89	0.01	1.15	1.09	-4.69	1.06	-0.43	-2.94	0.49	
11.0	-1.95	0.0	0.1708	0.038	0.0035	-0.0019	0.0025	0.000426	8.16	-3.24	-0.02	0.55	-0.67	6.75	9.89	0.01	1.15	1.09	-4.69	1.06	-0.43	-2.94	0.49	
12.0	-1.95	0.0	0.1741	0.0639	0.0033	-0.0010	0.0027	0.000468	8.84	-3.63	0.15	0.46	-0.82	6.71	10.42	-0.38	1.73	1.24	-5.77	1.20	-0.45	-3.16	0.50	
13.0	-2.0	0.0	0.1814	0.074	0.0035	-0.0009	0.0027	0.000536	9.35	-4.57	0.21	0.77	-0.98	7.21	10.82	-0.24	2.03	1.51	-7.02	1.50	-0.58	-3.42	0.70	
14.0	-2.00	0.0	0.1849	0.061	0.0036	-0.0008	0.0028	0.000594	9.89	-4.48	0.38	0.85	-1.06	7.29	11.29	-0.32	2.11	1.45	-8.18	1.36	-0.61	-3.79	0.75	
Part (6) $\bar{B}_{1,s} = 2^\circ$																								
4.0	-0.80	2.0	0.1128	0.0245	-0.0011	-0.0002	0.0004	0.000027	4.16	-0.86	-0.13	1.80	-0.02	3.09	2.89	0.21	0.54	0.66	2.72	0.39	-0.05	-0.36	0.05	
5.0	-1.00	2.0	0.1286	0.0253	-0.0011	-0.0003	0.0007	0.000085	4.99	-1.35	0.03	1.75	-0.11	3.79	4.09	0.10	0.80	0.62	1.69	0.42	-0.10	-0.76	0.04	
6.0	-1.15	2.0	0.1366	0.0288	-0.0005	-0.0009	0.0011	0.000182	5.65	-1.50	0.09	1.84	-0.18	4.24	5.01	0.15	1.14	0.93	1.9	0.60	-0.15	-1.12	0.10	
6.0	0.0	2.0	0.1366	0.0264	0.0013	0.0010	0.0005	0.000180	5.65	-1.44	0.09	1.84	-0.18	4.24	5.01	0.15	1.14	0.93	1.9	0.60	-0.15	-1.12	0.10	
7.0	0.0	2.0	0.1430	0.0279	0.0025	0.0006	0.0024	0.000254	6.41	-1.64	0.05	1.96	-0.23	4.79	6.09	0.41	2.19	0.98	-0.57	0.84	-0.24	-1.68	0.21	
8.0	0.0	2.0	0.1511	0.0313	0.0027	0.0005	0.0023	0.000317	7.32	-1.88	0.11	1.95	-0.34	5.20	6.94	0.24	2.76	1.08	-1.06	1.01	-0.35	-1.95	0.18	
9.0	0.0	2.0	0.1584	0.0352	0.0029	0.0012	0.0025	0.000396	8.22	-1.09	0.10	2.06	-0.37	5.34	7.48	0.26	3.08	1.18	-3.31	1.12	-0.47	-2.34	0.18	
10.0	0.0	2.0	0.1674	0.0367	0.0030	0.0016	0.0026	0.000494	8.87	-1.42	0.20	2.10	-0.49	5.55	8.11	0.03	3.28	1.21	-4.93	1.28	-0.44	-2.61	0.24	
11.0	0.0	2.0	0.1759	0.0407	0.0041	0.0017	0.0028	0.000528	9.40	-1.79	0.42	2.15	-0.70	5.77	9.00	-0.01	3.93	1.21	-6.18	1.49	-0.69	-3.08	0.24	
12.0	0.0	2.0	0.1796	0.0401	0.0039	0.0019	0.0028	0.000562	10.15	-2.02	0.29	2.27	-0.75	6.15	9.25	-0.12	3.57	1.29	-7.47	1.39	-0.70	-3.22	0.30	
13.0	0.0	2.0	0.1790	0.0398	0.0043	0.0023	0.0028	0.000565	10.40	-2.65	0.66	2.28	-0.72	6.43	9.59	-0.25	4.65	0.98	-8.71	1.88	-0.81	-3.67	0.34	
14.0	0.0	2.0	0.1843	0.0417	0.0043	0.0027	0.0045	0.000714	11.08	-2.89	0.60	2.38	-0.86	6.59	9.97	-0.22	4.76	1.14	-10.00	2.19	-0.84	-3.78	0.36	
Part (7) $\bar{B}_{1,s} = 6^\circ$																								
6.0	-0.95	6.0	0.1137	0.0138	-0.0002	0.0013	-0.0033	0.000170	5.69	-0.81	0.00	0.88	-0.08	3.58	0.03	0.21	1.04	0.66	0.65	0.37	-0.09	-0.26	0.04	
7.0	-1.35	6.0	0.1296	0.0149	0.0001	0.0004	-0.0014	0.000251	6.39	-1.53	0.13	0.59	-0.17	3.85	0.92	0.18	0.93	0.85	-0.58	0.47	-0.08	-0.54	0.00	
8.0	-1.75	6.0	0.1326	0.0165	0.0007	0.0009	-0.0027	0.000500	7.23	-1.88	0.15	0.54	-0.28	4.39	1.75	0.01	1.17	0.86	-1.76	0.57	-0.15	-0.93	0.02	
9.0	-1.95	6.0	0.1406	0.0167	0.0018	0.0007	-0.0024	0.000567	8.03	-2.54	0.09	0.90	-0.21	4.80	2.12	0.03	1.40	0.86	-2					

TABLE V. - ROTOR CHARACTERISTICS AT A TIP-SPEED RATIO OF APPROXIMATELY 0.5 - Continued

(d)  $\alpha_s = 6^\circ$ ; fuselage on

Nominal control, deg			Aerodynamic characteristics							Feathering motion, deg					Flapping motion, deg					In-plane motion, deg				
$\bar{A}_{0,s}$	$\bar{A}_{1,s}$	$\bar{B}_{1,s}$	$C_L$	$C_D$	$C_m$	$C_l$	$C_y$	$C_q$	$A_{0,s}$	$A_{1,s}$	$A_{2,s}$	$B_{1,s}$	$B_{2,s}$	$a_{0,s}$	$a_{1,s}$	$a_{2,s}$	$b_{1,s}$	$b_{2,s}$	$E_0$	$E_1$	$E_2$	$F_1$	$F_2$	
Part (1) $\bar{B}_{1,s} = -4^\circ$																								
6.0°	-0.4°	-4.0	0.1177A	0.0523	0.0015	-0.0002	-0.0001	0.00015B	5.97	-1.52	-0.01	-3.62	-0.54	5.17	12.65	0.12	0.78	1.22	0.48	0.79	-0.33	-2.74	0.72	
7.0°	-0.6°	-4.0	0.1064	0.0555	0.0024	-0.0003	0.0004	0.000200	6.24	-1.56	0.01	-3.40	-0.73	5.47	13.38	0.21	0.07	1.35	-0.77	0.70	-0.39	-3.21	0.96	
8.0°	-0.7°	-4.0	0.1716	0.0572	0.0031	0.0001	-0.0009	0.000269	7.23	-2.11	0.01	-3.43	-0.93	5.63	13.89	0.09	1.04	1.31	-2.24	1.05	-0.55	-3.39	0.89	
9.0°	-0.8°	-4.0	0.1777A	0.0622	0.0031	0.0001	-0.0001	0.000316	8.17	-2.68	0.01	-3.21	-0.93	6.04	14.62	-0.05	0.64	1.36	-3.57	0.96	-0.65	-3.90	1.08	
Part (2) $\bar{B}_{1,s} = 0^\circ$																								
6.0°	-0.8°	0.0	0.1346	0.0404	-0.0007	-0.0002	0.0002	0.000147	5.88	-1.44	-0.08	0.15	-0.21	4.96	7.92	0.22	0.88	0.99	0.19	0.53	-0.25	-1.78	0.26	
7.0°	-0.9°	0.0	0.1192	0.0424	-0.0007	-0.0002	0.0002	0.000210	6.70	-1.71	0.00	0.21	-0.21	4.86	8.10	0.38	1.84	1.32	-0.84	0.69	-0.27	-2.02	0.58	
8.0°	-1.10	0.0	0.1113	0.0441	-0.0007	-0.0002	0.0002	0.000250	7.42	-2.09	0.01	0.33	-0.23	5.21	9.24	0.50	1.14	1.28	-2.54	0.94	-0.44	-2.38	0.43	
9.0°	-1.40	0.0	0.1075	0.0457	-0.0011	-0.0006	0.0001	0.000345	8.04	-2.57	0.00	0.48	-0.24	5.43	9.91	0.65	1.15	1.32	-3.44	0.97	-0.58	-2.62	0.51	
10.0°	-1.50	0.0	0.1171	0.0473	-0.0019	-0.0005	-0.0018	0.000412	8.50	-3.01	0.01	0.44	-0.15	5.41	10.46	0.31	1.25	1.41	-4.70	1.08	-0.45	-3.00	0.57	
11.0°	-1.50	0.0	0.1198	0.0475	-0.0015	-0.0004	-0.0016	0.000471	9.63	-3.77	0.01	0.55	-0.52	5.68	11.08	-0.06	1.64	1.41	-6.21	1.02	-0.50	-3.46	0.51	
12.0°	-1.6°	0.0	0.1256	0.0410	-0.0023	-0.0009	-0.0030	0.000540	10.24	-3.96	0.01	0.55	-1.03	5.84	11.96	0.00	1.97	1.45	-7.63	1.47	-0.61	-3.83	0.57	
Part (3) $\bar{B}_{1,s} = 2^\circ$																								
6.0°	-0.50	2.0	0.1569	0.0291	-0.0004	0.0001	-0.0002	0.000154	5.81	-1.12	0.06	1.93	-0.25	4.15	5.07	0.18	0.82	1.03	0.47	0.58	-0.14	-1.02	0.10	
7.0°	-1.10	2.0	0.1476	0.0312	-0.0007	0.0005	-0.0017	0.000216	6.59	-1.52	0.04	2.07	-0.23	4.75	5.87	0.23	0.75	1.32	-0.64	0.68	-0.24	-1.40	0.12	
8.0°	-1.20	2.0	0.1464	0.0331	-0.0008	0.0004	-0.0014	0.000283	7.35	-1.95	0.09	2.14	-0.41	5.12	6.77	0.25	1.19	1.21	-1.94	0.90	-0.19	-1.93	0.07	
9.0°	-1.40	2.0	0.1555	0.0367	-0.0006	0.0009	-0.0028	0.000347	8.17	-2.28	0.19	2.25	-0.51	5.31	7.54	-0.07	1.01	1.51	-3.90	0.81	-0.34	-2.07	0.21	
10.0°	-1.65	2.0	0.1687	0.0404	-0.0007	0.0008	-0.0026	0.000414	8.94	-2.83	0.27	2.40	-0.73	5.59	8.23	-0.44	1.30	1.63	-4.85	0.99	-0.58	-2.59	0.28	
11.0°	-1.75	2.0	0.1716	0.0419	-0.0005	0.0007	-0.0024	0.000485	9.75	-3.15	0.27	2.60	-0.61	6.18	8.87	-0.20	1.45	1.60	-6.06	1.14	-0.42	-2.73	0.41	
12.0°	-1.90	2.0	0.1780	0.0457	-0.0011	0.0006	-0.0021	0.000540	10.06	-3.65	0.27	2.62	-0.53	6.40	9.53	-0.44	1.97	1.77	-7.20	1.27	-0.42	-3.08	0.50	
13.0°	-1.95	2.0	0.1791	0.0467	-0.0011	0.0011	-0.0025	0.000592	10.80	-4.20	0.55	2.74	-1.03	6.57	10.01	-0.51	1.81	1.76	-8.13	1.45	-0.55	-3.50	0.46	
Part (4) $\bar{B}_{1,s} = 6^\circ$																								
6.0°	-0.70	6.0	0.1204	0.0138	-0.0014	0.0002	-0.0014	0.000137	5.05	-0.48	-0.06	5.81	-0.63	2.79	-0.72	0.16	0.87	0.77	1.36	0.23	-0.02	0.00	0.04	
7.0°	-0.85	6.0	0.1162	0.0160	-0.0016	-0.0005	-0.0014	0.000170	5.77	-0.91	0.14	5.87	-0.23	3.21	1.12	-0.17	1.23	0.99	1.18	0.40	-0.06	-0.23	-0.02	
8.0°	-1.20	6.0	0.1269	0.0183	-0.0015	-0.0001	0.0000	0.000239	6.66	-1.15	0.08	5.73	-0.41	3.86	1.02	0.08	1.26	1.03	-0.77	0.54	-0.12	-0.68	-0.01	
9.0°	-1.55	6.0	0.1460	0.0206	-0.0017	-0.0001	0.0002	0.000294	7.54	-1.59	0.20	6.03	-0.11	4.22	1.64	0.21	1.24	1.09	-1.97	0.65	-0.14	-0.99	0.04	
10.0°	-1.85	6.0	0.1546	0.0209	-0.0005	0.0005	0.0005	0.000362	8.08	-2.15	0.26	6.11	-0.11	4.57	2.76	0.12	1.39	1.19	-3.12	0.97	-0.35	-1.33	0.05	
11.0°	-1.95	6.0	0.1614	0.0238	-0.0005	0.0005	0.0006	0.000430	8.57	-2.62	0.50	6.17	-0.21	4.83	3.69	-0.06	1.71	1.55	-4.44	0.88	-0.28	-1.65	0.02	
12.0°	-2.00	6.0	0.1612	0.0276	-0.0005	0.0005	0.0010	0.000483	9.70	-3.02	0.17	6.34	-0.41	5.06	4.11	0.05	1.95	1.54	-5.88	1.05	-0.57	-1.65	0.10	
13.0°	-2.10	6.0	0.1773	0.0293	-0.0005	0.0001	-0.0004	0.000597	10.13	-3.54	0.32	6.36	-0.31	5.51	4.75	-0.15	1.96	1.51	-6.97	1.23	-0.45	-2.28	0.14	
14.0°	-2.60	6.0	0.1842	0.0354	-0.0018	0.0000	-0.0005	0.000633	10.86	-4.27	0.47	6.36	-0.51	5.70	5.07	-0.15	2.05	1.59	-8.58	1.49	-0.45	-2.28	0.09	
14.0°	-2.65	6.0	0.1844	0.0382	-0.0019	0.0001	-0.0012	0.000661	11.47	-4.36	0.41	6.73	-0.63	6.06	5.76	-0.19	2.50	1.51	-9.57	1.56	-0.56	-2.67	0.05	
15.0°	-1.40	6.0	0.1705	0.0435	-0.0020	0.0010	-0.0012	0.000703	12.00	-3.46	0.42	6.57	-0.81	5.98	6.12	-0.01	4.12	1.79	-10.85	1.84	-0.60	-2.97	0.00	
Part (5) $\bar{B}_{1,s} = 6^\circ$ (check tests)																								
11.0°	-0.50	6.0	0.1607	0.0249	0.0000	0.0001	-0.0006	0.000476	9.70	-3.00	0.24	6.42	-0.41	5.09	4.18	0.00	1.45	1.71	-5.63	1.00	-0.29	-1.81	0.18	
12.0°	-0.50	6.0	0.1650	0.0279	0.0000	0.0006	-0.0019	0.000592	10.46	-3.53	0.32	6.50	-0.61	5.37	5.01	-0.23	1.73	1.50	-7.10	1.04	-0.33	-2.12	0.14	
13.0°	-0.55	6.0	0.1655	0.0299	-0.0008	0.0005	-0.0018	0.000596	10.98	-3.85	0.45	6.52	-0.41	5.81	5.27	-0.23	1.99	1.76	-8.68	1.37	-0.37	-2.20	0.04	
14.0°	-0.15	6.0	0.1616	0.0275	-0.0014	0.0011	-0.0033	0.000468	11.46	-3.78	0.31	6.72	-0.51	6.20	6.52	-0.39	2.69	1.51	-9.77	1.55	-0.57	-2.63	0.10	
14.0°	-2.10	6.0	0.1607	0.0435	-0.0020	0.0021	-0.0001	0.000718	12.03	-4.19	0.39	6.52	-0.71	6.06	6.07	-0.81	3.43	1.50	-10.92	1.74	-0.65	-2.85	0.11	
16.0°	-1.90	6.0	0.1816	0.0448	-0.0007	0.0015	-0.0041	0.000773	12.66	-4.09	0.37	6.73	-0.91	6.15	6.84	-0.74	3.74	1.60	-12.45	1.82	-0.65	-3.12	0.04	

TABLE V.- ROTOR CHARACTERISTICS AT A TIP-SPEED RATIO OF APPROXIMATELY 0.5 - Continued

(e)  $\alpha_0 = 12^\circ$ ; no fuselage

Nominal control, deg			Aerodynamic characteristics							Feathering motion, deg					Flapping motion, deg					In-plane motion, deg				
$\bar{A}_{0,s}$	$\bar{A}_{1,s}$	$\bar{B}_{1,s}$	$C_L$	$C_D$	$C_M$	$C_1$	$C_Y$	$C_Q$	$A_{0,s}$	$A_{1,s}$	$A_{2,s}$	$B_{1,s}$	$B_{2,s}$	$a_{0,s}$	$a_{1,s}$	$a_{2,s}$	$b_{1,s}$	$b_{2,s}$	$E_0$	$E_1$	$E_2$	$F_1$	$F_2$	
Part (1) $\bar{B}_{1,s} = -4^\circ$																								
6.0	-0.10	4.0	0.1726	0.0758	0.0041	0.0000	-0.0006	0.000111	4.43	-0.87	0.16	-3.64	-0.63	6.84	13.31	-0.27	1.58	1.25	1.11	1.00	-0.65	-3.50	0.85	
7.0	-0.30	4.0	0.1768	0.0781	0.0048	0.0004	-0.0016	0.000194	6.42	-1.22	0.16	-3.58	-0.72	7.32	14.32	-0.61	1.78	1.12	-1.15	1.19	-1.17	-3.66	0.82	
8.0	-0.55	4.0	0.1849	0.0819	0.0066	0.0008	-0.0030	0.000294	7.00	-1.70	0.19	-3.46	-0.93	7.42	14.63	-0.64	2.17	1.16	-1.55	1.41	-1.91	-4.10	1.09	
9.0	-0.85	4.0	0.1891	0.0840	0.0074	0.0014	-0.0047	0.000332	7.84	-1.90	0.44	-3.35	-1.11	7.51	15.30	-1.25	2.72	1.69	-2.93	1.56	-1.05	-4.60	1.02	
10.0	-1.35	4.0	0.1906	0.0868	0.0073	0.0009	-0.0024	0.000404	8.26	-2.55	0.51	-3.25	-1.24	7.59	15.23	-1.00	3.26	1.09	-4.00	1.69	-0.96	-4.78	1.18	
Part (2) $\bar{B}_{1,s} = -3^\circ$																								
6.0	-0.90	-3.0	0.1783	0.0739	0.0037	0.0001	-0.0009	0.000144	5.27	-1.55	0.24	-2.75	-0.70	6.14	12.24	-0.56	1.41	1.12	0.43	1.18	-0.51	-3.10	0.60	
7.0	-0.95	-1.0	0.1819	0.0776	0.0040	0.0005	-0.0021	0.000206	5.81	-2.01	0.07	-2.51	-0.93	7.28	13.27	-0.04	0.79	1.69	-0.79	1.27	-0.54	-3.51	0.88	
8.0	-1.30	-1.0	0.1884	0.0802	0.0042	0.0010	-0.0035	0.000279	6.80	-2.54	0.21	-2.36	-0.99	7.09	13.87	-0.58	1.38	1.50	-2.17	1.53	-0.73	-3.87	0.72	
9.0	-1.55	-1.0	0.1924	0.0820	0.0042	0.0012	-0.0052	0.000351	7.40	-2.90	0.21	-2.25	-1.09	7.09	14.50	-0.58	1.38	1.50	-2.17	1.53	-0.73	-3.87	0.72	
10.0	-1.45	-1.0	0.1943	0.0836	0.0059	0.0013	-0.0045	0.000430	8.02	-3.57	0.45	-2.06	-1.31	7.68	14.93	-1.14	1.79	1.14	-3.20	1.56	-0.81	-4.70	0.92	
11.0	-1.60	-3.0	0.1973	0.0874	0.0053	0.0018	-0.0059	0.000492	8.60	-4.10	0.54	-1.89	-1.42	7.95	15.04	-1.20	1.87	1.22	-6.43	1.57	-0.91	-4.69	1.01	
Part (3) $\bar{B}_{1,s} = -2^\circ$																								
6.0	-0.70	-2.0	0.1698	0.0678	0.0019	-0.0002	0.0000	0.000122	5.59	-1.22	0.05	-1.63	-0.59	6.16	10.75	-0.12	0.66	1.42	1.16	1.00	-0.45	-2.66	0.60	
7.0	-0.85	-2.0	0.1727	0.0720	0.0021	0.0003	-0.0014	0.000195	6.30	-1.67	0.03	-1.64	-0.63	6.79	11.55	0.00	1.27	1.34	-0.35	1.15	-0.45	-3.20	0.64	
8.0	-1.00	-2.0	0.1776	0.0776	0.0018	0.0001	-0.0018	0.000266	7.11	-2.09	-0.01	-1.58	-0.88	7.12	12.53	0.26	1.18	1.44	-1.42	1.04	-0.53	-3.70	0.92	
9.0	-1.00	-2.0	0.1820	0.0781	0.0028	0.0007	-0.0024	0.000357	7.84	-2.49	0.28	-1.45	-0.99	6.88	12.55	-0.53	1.84	1.47	-2.90	1.42	-0.60	-3.83	0.83	
10.0	-1.10	-2.0	0.1911	0.0795	0.0035	0.0012	-0.0037	0.000410	8.40	-3.12	0.27	-1.25	-1.22	7.58	13.46	-0.61	1.89	1.52	-4.53	1.43	-0.69	-4.06	1.05	
11.0	-1.35	-2.0	0.1943	0.0813	0.0041	0.0009	-0.0034	0.000475	9.28	-3.85	0.59	-1.24	-1.22	7.64	13.94	-0.89	2.78	1.60	-5.68	1.93	-0.85	-4.29	0.86	
12.0	-1.40	-2.0	0.1951	0.0831	0.0059	0.0015	-0.0050	0.000533	9.48	-4.10	0.76	-1.24	-1.38	7.85	14.16	-1.15	3.23	0.98	-6.68	2.11	-0.90	-4.63	1.01	
Part (4) $\bar{B}_{1,s} = 0^\circ$																								
6.0	-0.95	0.0	0.1615	0.0599	0.0011	-0.0003	0.0008	0.000140	5.50	-1.41	0.11	0.11	-0.46	6.18	8.90	0.14	1.20	1.25	0.96	0.93	-0.18	-2.16	0.28	
7.0	-1.20	0.0	0.1679	0.0622	0.0009	0.0000	-0.0004	0.000194	6.39	-1.93	0.15	0.28	-0.51	6.30	9.59	-0.14	0.68	1.28	-0.17	0.84	-0.35	-2.65	0.37	
8.0	-1.45	0.0	0.1733	0.0651	0.0006	0.0000	-0.0018	0.000266	7.10	-2.49	0.09	0.46	-0.62	6.76	10.23	0.11	1.29	1.38	-1.89	1.17	-0.48	-2.91	0.54	
9.0	-1.55	0.0	0.1795	0.0671	0.0029	0.0004	-0.0015	0.000355	7.87	-2.84	0.20	0.44	-0.82	6.91	10.74	0.10	0.95	1.61	-2.87	1.06	-0.55	-3.35	0.54	
10.0	-1.55	0.0	0.1856	0.0777	0.0042	0.0003	-0.0019	0.000404	8.45	-3.13	0.12	0.71	-0.88	6.99	10.69	-0.08	1.70	1.70	-4.68	1.17	-0.52	-3.46	0.63	
11.0	-1.75	0.0	0.1890	0.0699	0.0042	0.0005	-0.0024	0.000477	9.06	-3.69	0.22	0.68	-1.02	7.23	11.62	-0.35	2.37	1.59	-5.98	1.59	-0.71	-3.80	0.66	
12.0	-1.85	0.0	0.1929	0.0740	0.0051	0.0007	-0.0026	0.000541	9.41	-4.40	0.51	0.75	-1.15	7.45	12.21	-0.54	2.84	1.51	-7.24	2.24	-0.83	-4.04	0.77	
Part (5) $\bar{B}_{1,s} = 2^\circ$																								
6.0	-1.15	2.0	0.1598	0.0513	0.0010	0.0000	0.0001	0.000147	5.55	-1.41	0.08	2.03	-0.28	6.06	6.68	0.16	0.97	1.21	0.62	0.82	-0.28	-1.88	0.23	
7.0	-1.35	2.0	0.1637	0.0559	0.0006	-0.0002	0.0004	0.000202	6.29	-2.00	0.14	2.10	-0.44	6.07	7.40	0.00	1.24	1.47	-0.62	1.02	-0.45	-2.28	0.21	
8.0	-1.60	2.0	0.1722	0.0571	0.0021	0.0001	-0.0007	0.000276	7.10	-2.58	0.18	2.18	-0.51	6.51	8.11	-0.16	1.05	1.26	-2.07	0.95	-0.35	-2.39	0.21	
9.0	-1.70	2.0	0.1776	0.0595	0.0021	0.0002	-0.0006	0.000355	7.80	-2.77	0.54	2.21	-0.59	6.71	8.83	-0.58	1.46	1.21	-3.29	1.12	-0.52	-2.68	0.24	
10.0	-2.00	2.0	0.1819	0.0618	0.0023	0.0005	-0.0020	0.000410	8.42	-3.29	0.36	2.40	-0.75	7.03	9.14	-0.52	1.58	1.51	-4.41	1.35	-0.57	-3.09	0.27	
11.0	-2.10	2.0	0.1847	0.0638	0.0026	0.0005	-0.0018	0.000474	8.87	-3.88	0.27	2.71	-0.85	7.45	9.63	-0.26	1.45	1.44	-5.52	1.93	-0.55	-3.36	0.49	
12.0	-2.20	2.0	0.1889	0.0648	0.0030	0.0002	-0.0016	0.000534	9.44	-4.21	0.56	2.73	-0.92	7.53	10.00	-0.91	1.82	1.44	-6.98	1.93	-0.55	-3.64	0.49	
13.0	-2.30	2.0	0.1912	0.0663	0.0026	0.0010	-0.0032	0.000606	10.00	-4.93	0.71	2.60	-0.98	7.52	10.43	-1.05	2.91	1.18	-8.24	2.14	-0.70	-3.88	0.47	
Part (6) $\bar{B}_{1,s} = 4^\circ$																								
6.0	-1.30	4.0	0.1477	0.0427	0.0000	-0.0003	0.0010	0.000140	5.53	-1.54	0.00	3.97	-0.17	5.50	4.44	0.14	0.82	1.14	0.68	0.75	-0.21	-1.59	0.08	
7.0	-1.65	4.0	0.1528	0.0443	0.0008	0.0000	-0.0003	0.000212	6.11	-2.11	0.13	4.06	-0.28	5.73	5.18	-0.07	0.98	1.22	-0.69	0.85	-0.25	-1.82	0.04	
8.0	-1.85	4.0	0.1644	0.0468	0.0010	0.0001	-0.0001	0.000268	6.91	-2.47	0.17	4.05	-0.36	6.10	5.95	-0.02	1.17	1.15	-2.14	0.86	-0.27	-2.15	0.15	
9.0	-2.10	4.0	0.1707	0.0492	0.0019	0.0003	-0.0013	0.000356	7.15	-2.95	0.15	4.14	-0.46	6.78	6.36	-0.17	1.35	1.28	-3.52	1.01	-0.35	-2.29	0.18	
10.0	-2.20	4.0	0.1758	0.0515	0.0014	0.0004	-0.0012	0.000422	8.48	-3.51	0.41	4.24	-0.77	6.63	7.19	-0.46	1.60	1.29	-4.70	1.30	-0.45	-2.60	0.10	
11.0	-2.40	4.0	0.1840	0.0548	0.0020	0.0002	-0.0010	0.000484	9.00	-3.81	0.33	4.46	-0.46	7.26	7.72	-0.28	1.70	1.44	-5.73	1.29	-0.44	-2.66	0.21	
12.0	-2.40	4.0	0.1832	0.0561	0.0020	0.0002	-0.0009	0.000559	9.45	-4.30	0.58	4.46	-0.57	7.06	7.93	-0.57	2.32	1.16	-7.28	1.72	-0.51	-3.09	0.23	
13.0	-2.55	4.0	0.1884	0.0590	0.0011	0.0007	-0.0025	0.000608	10.08	-4.84	0.70	4.54	-0.77	7.29	8.43	-0.72	2.92	1.45	-8.31	1.80	-0.65	-3.48	0.23	
Part (7) $\bar{B}_{1,s} = 6^\circ$																								
5.0	-1.00	6.0	0.1366	0.0358	-0.0015	0.0000	0.0001	0.000112	4.62	-0.85	0.05	5.65	-0.18	4.51	1.32	0.37	1.31	0.93	1.45	0.64	-0.10	-0.65	-0.01	
6.0	-1.30	6.0	0.1433	0.0390	-0.0006	-0.0002	0.0004	0.000166	5.09	-1.46	0.05	5.84	-0.14	4.89	1.73	0.20	1.15	0.96	0.64	0.71	-0.21	-0.90	0.08	
7.0	-1.60	6.0	0.1519	0.0377	-0.0002	-0.0002	0.0005	0.000234	6.13	-1.82	0.08	5.99	-0.11	5.23	2.11	0.32	1.09	1.31	-0.72	0.99	-0.18	-1.15	0.00	
8.0	-1.80	6.0	0.1582	0.0402	0.0001	0.0003	-0.0007	0.000297	6.97	-2.19	0.16	6.03	-0.14	5.48	3.35	0.13	1.27	1.12	-2.06	1.00	-0.24	-1.58	-0.01	
9.0	-2.10	6.0	0.1655	0.0428	0.0004	0.0003	-0.0005	0.000362	7.74	-2.58	0.18	6.32	-0.14	6.18	4.49	0.13	1.44	1.32	-3.35	1.07	-0.32	-2.10	0.07	
10.0	-2.30	6.0	0.1714	0.0454	0.0004	0.0000	-0.0005	0.000427	8.59	-2.95	0.20	6.44	-0.25	6.26	4.67	0.01	1.90	1.38	-4.68	1.25	-0.34	-2.24	0.07	
11.0	-2.50	6.0	0.1774	0.0481	0.0005	-0.0001	-0.0001	0.000491	9.10	-3.58	0.34	6.55	-0.38	6.70	5.19	-0.33	1.70	1.32	-5.68	1.29	-0.40	-2.58	0.01	
12.0	-2.60	6.0	0.1807	0.0501	0.0005	0.0004	-0.0016	0.000597	9.63	-4.														

TABLE V. - ROTOR CHARACTERISTICS AT A TIP-SPEED RATIO OF APPROXIMATELY 0.3 - Concluded

(r)  $\alpha_g = 12^\circ$ ; fuselage on

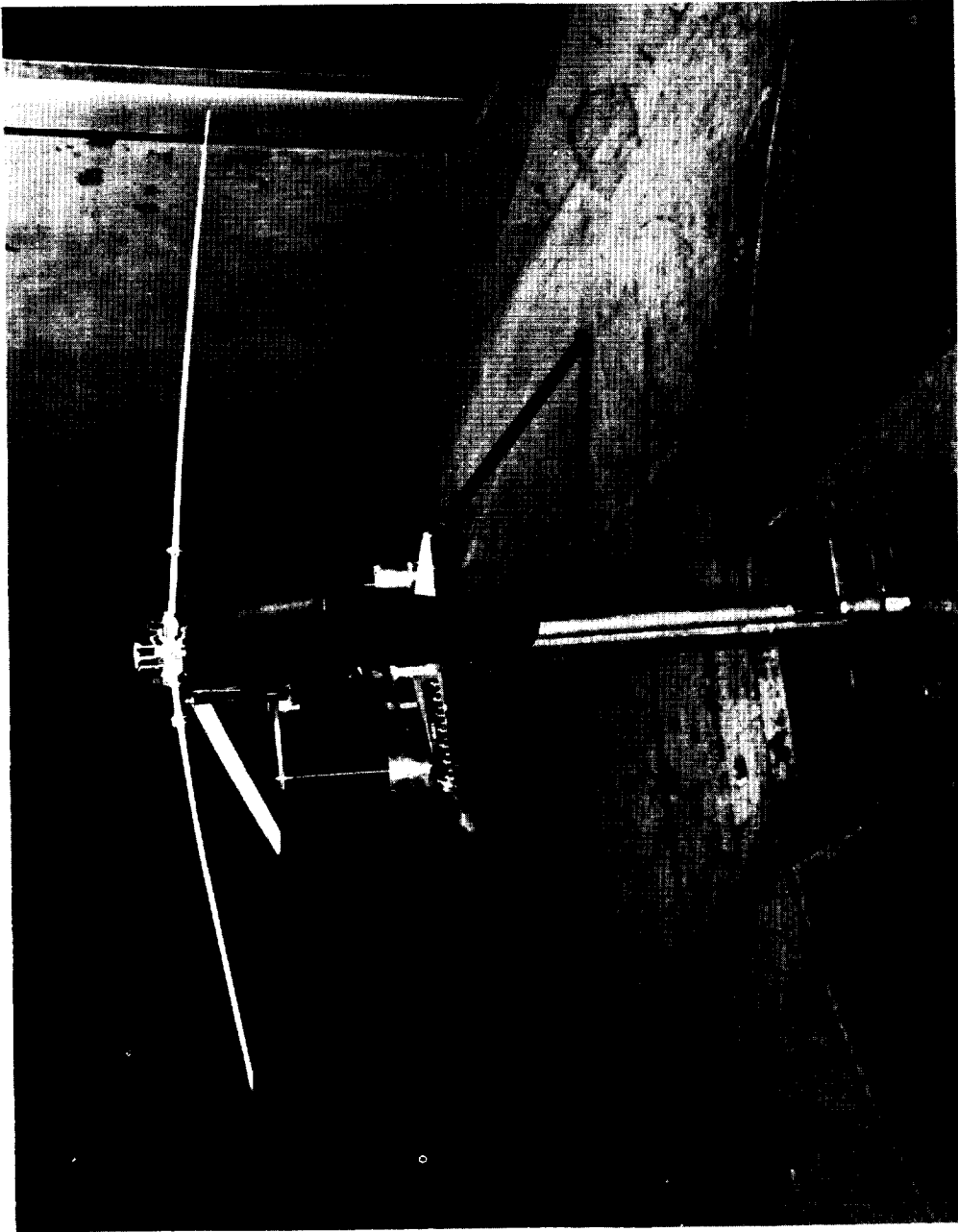
Nominal control, deg			Aerodynamic characteristics							Feathering motion, deg					Flapping motion, deg					In-plane motion, deg				
$\bar{A}_{0,s}$	$\bar{A}_{1,s}$	$\bar{B}_{1,s}$	$C_L$	$C_D$	$C_m$	$C_{L1}$	$C_{Y1}$	$C_Q$	$A_{0,s}$	$A_{1,s}$	$A_{2,s}$	$B_{1,s}$	$B_{2,s}$	$a_{0,s}$	$a_{1,s}$	$a_{2,s}$	$b_{1,s}$	$b_{2,s}$	$E_0$	$E_1$	$E_2$	$F_1$	$F_2$	
Part (1) $\bar{B}_{1,s} = -2^\circ$																								
7.0°	-0.10	-1.0	0.1744	0.0774	0.0008	-0.0001	0.0003	0.000186	6.97	-1.51	0.10	-1.70	-0.2	5.89	12.42	-0.10	1.19	1.47	-0.37	1.04	-0.49	-3.22	0.59	
8.0°	-1.0	-2.0	0.1792	0.0777	0.0024	0.0001	-0.0009	0.000256	7.31	-2.35	.12	-1.40	-1.0	6.53	13.28	.20	1.70	1.78	-1.78	1.13	-1.47	-3.65	.89	
9.0°	-1.10	-3.0	0.1847	0.0816	0.0041	0.0007	-0.0022	0.000350	8.04	-2.72	.22	-1.47	-1.2	6.63	14.02	-0.02	1.58	1.65	-3.43	1.52	-1.56	-3.84	.86	
10.0°	-1.20	-4.0	0.1892	0.0832	0.0052	0.0010	-0.0035	0.000403	8.87	-3.30	.32	-1.28	-1.5	6.72	14.44	-0.44	1.76	1.80	-4.87	1.44	-1.64	-4.18	.96	
11.0°	-1.30	-5.0	0.1934	0.0849	0.0059	0.0010	-0.0054	0.000462	9.47	-3.69	.52	-1.23	-1.1	6.83	15.05	-0.76	1.99	1.67	-6.11	1.16	-1.94	-4.18	.99	
Part (2) $\bar{B}_{1,s} = 0^\circ$																								
7.0°	-0.10	0.0	0.1642	0.0655	0.0002	-0.0005	0.0009	0.000120	5.90	-1.45	-0.03	0.30	-0.43	5.40	9.04	0.65	0.40	1.63	0.56	0.82	-0.25	-2.28	0.58	
7.0°	-1.0	0.0	0.1679	0.0659	0.0015	0.0000	-0.0004	0.000196	6.67	-2.05	.12	.26	-1.14	5.71	10.28	.20	1.23	1.61	-1.12	1.12	-1.44	-2.57	.50	
7.0°	-1.40	0.0	0.1744	0.0681	0.0015	0.0004	-0.0017	0.000264	7.52	-2.39	.15	.28	-1.75	5.83	11.04	-0.15	1.09	1.61	-2.35	1.24	-1.45	-3.08	.53	
9.0°	-1.10	0.0	0.1841	0.0697	0.0021	0.0003	-0.0014	0.000324	8.04	-2.96	.25	.37	-1.9	5.92	11.62	-0.09	1.59	1.57	-3.48	1.45	-1.51	-3.35	.60	
10.0°	-1.00	0.0	0.1888	0.0709	0.0017	0.0002	-0.0012	0.000403	8.73	-3.40	.30	.60	-1.4	6.37	12.08	-0.18	1.83	1.70	-4.73	1.55	-1.58	-3.69	.63	
11.0°	-1.10	0.0	0.1904	0.0714	0.0024	0.0007	-0.0026	0.000471	9.45	-3.99	.45	.17	-1.1	6.29	12.14	-0.71	3.40	1.55	-6.18	2.12	-1.80	-3.72	.53	
11.0°	-1.10	0.0	0.1945	0.0774	0.0031	0.0007	-0.0024	0.000558	10.05	-4.15	.58	.69	-1.0	7.23	13.10	-1.15	3.10	1.29	-7.74	1.84	-1.70	-4.25	.64	

TABLE VI.- ROTOR-BLADE MOTIONS AFTER A SUDDEN CONTROL INCREMENT; NO FUSELAGE

Initial nominal control, deg			Pulse time, $t_1$ , cycles	First complete revolution after control motion		Cycle analyzed		Feathering motion, deg					Flapping motion, deg					In-plane motion, deg						
$\bar{A}_{0,s}$	$\bar{A}_{1,s}$	$\bar{B}_{1,s}$		$\beta_{\psi}$ , deg ( $\psi = 0^\circ$ )	$\beta_{\psi}$ , deg ( $\psi = 180^\circ$ )	Number after control motion	Sec/rev	$\beta_{\psi}$ , deg ( $\psi = 0^\circ$ )	$\beta_{\psi}$ , deg ( $\psi = 180^\circ$ )	$A_{0,s}$	$A_{1,s}$	$A_{2,s}$	$B_{1,s}$	$B_{2,s}$	$a_{0,s}$	$a_{1,s}$	$a_{2,s}$	$b_{1,s}$	$b_{2,s}$	$E_0$	$E_1$	$E_2$	$F_1$	$F_2$
(a) $\alpha_B = 0^\circ; \Delta\bar{A}_{0,s} = 4^\circ$																								
9.05	0	4.0	2.8	-----	-----	4	0.0900	-2.4	14.4	11.72	-1.53	0.50	4.08	-0.63	6.22	8.67	0.17	4.59	1.14	-5.69	1.26	-0.55	-3.16	0.20
10.05	0	4.0	2.9	-----	-----	4	0.0885	-2.7	14.9	12.43	-1.61	.26	4.20	-1.05	6.29	9.21	.07	4.60	1.25	-7.09	1.21	-.67	-3.50	.30
11.05	0	4.0	3.5	-----	-----	5	0.0920	-3.0	15.2	12.69	-2.46	.52	4.35	-.88	6.53	9.40	.27	5.64	1.28	-9.31	1.66	-.67	-3.65	.24
13.05	0	4.0	2.0	-----	-----	5	0.0850	-2.5	16.5	14.47	-2.46	.43	4.99	-1.18	6.93	9.81	-.24	5.36	1.42	-10.84	1.32	-.94	-4.28	.41
15.05	0	4.0	3.0	-----	-----	4	0.0860	-2.4	18.1	14.77	-3.41	.78	4.66	-1.50	7.60	10.55	-.48	6.54	1.21	-13.42	1.75	-1.43	-4.64	.55
(b) $\alpha_B = 6^\circ; \Delta\bar{A}_{0,s} = 4^\circ$																								
8.05	-1.00	4.0	1.4	-----	-----	4	0.0890	-14.3	26.6	10.64	-2.67	0.40	-2.50	-1.64	7.53	19.25	-0.54	0.66	2.17	-4.91	-0.59	-1.01	-6.38	1.73
9.05	-1.10	4.0	2.9	-----	-----	4	0.0890	-14.3	26.6	11.51	-3.36	.58	-2.39	-1.76	6.88	20.76	-.73	1.27	2.51	-6.70	.02	-1.05	-6.74	1.68
10.05	-1.15	4.0	2.4	-----	-----	4	0.0890	-14.3	26.7	11.85	-3.37	.69	-2.18	-1.77	7.10	20.41	-.45	2.64	2.35	-9.01	.11	-1.28	-6.85	1.32
11.05	-1.15	4.0	2.7	-----	-----	4	0.0950	-14.3	29.1	11.90	-4.14	.95	-2.00	-2.03	7.65	20.11	-.44	3.84	2.46	-10.61	.13	-1.30	-7.42	1.65
8.05	-1.65	0	.9	-----	-----	5	0.0975	-9.4	23.6	10.37	-5.95	.45	1.12	-1.43	7.26	16.06	.14	3.42	1.34	-6.12	1.55	-.92	-5.42	.72
10.05	-1.65	0	1.5	-----	-----	5	0.0890	-9.4	22.8	11.90	-4.44	.35	1.69	-1.63	7.53	15.63	.27	3.04	1.63	-7.25	1.55	-.96	-5.43	.63
12.05	-2.15	0	2.1	-----	-----	4	0.0905	-9.4	23.7	12.55	-6.35	1.08	1.60	-1.70	7.18	16.00	-.32	4.58	1.19	-11.42	1.54	-1.08	-6.00	1.23
8.05	-1.65	2.0	1.0	-----	-----	6	0.1020	-5.6	19.6	10.14	-5.99	.58	3.07	-1.06	7.13	12.69	-.22	4.25	1.05	-6.59	2.14	-.76	-4.93	.69
10.05	-2.05	2.0	.9	-----	-----	5	0.0965	-5.1	20.2	11.41	-5.10	.58	3.23	-1.45	7.59	12.61	-.27	4.40	1.45	-8.90	2.03	-.85	-5.46	.55
12.05	-2.40	2.0	2.0	-----	-----	4	0.0900	-4.8	20.9	12.74	-6.07	.67	3.36	-1.57	7.91	12.93	-.32	4.76	1.28	-10.87	1.96	-1.01	-5.35	.71
14.05	-2.70	2.0	1.5	-----	-----	5	0.0860	-4.9	21.4	13.47	-7.75	1.32	3.66	-1.68	7.65	13.14	-.90	4.76	1.31	-13.04	2.28	-1.00	-5.76	.63
(c) $\alpha_B = 0^\circ; \Delta\bar{A}_{0,s} = 2^\circ; \Delta\bar{B}_{1,s} = -4^\circ$																								
5.05	-0.60	-2.0	0.3	<-8.0	21.5	8	0.0900	-12.6	26.6	6.77	-1.59	0.24	-5.70	-1.01	6.90	18.70	-0.23	0.76	1.61	-1.34	0.30	-0.77	-4.65	1.26
6.05	-1.60	-2.0	.5	<-8.0	21.2	6	0.0865	-12.6	26.0	7.19	-2.36	.25	-5.47	-1.01	6.57	18.34	-.43	.01	1.75	-1.14	-.05	-.64	-4.75	1.48
7.05	-1.90	-2.0	.5	<-8.0	23.6	8	0.0900	-13.9	26.4	8.00	-2.39	.48	-5.21	-1.21	7.18	20.03	-.25	1.45	1.87	-3.74	.60	-1.07	-5.48	1.65
8.05	-1.10	-2.0	.5	<-8.0	24.2	7	0.0910	-13.9	26.6	9.11	-2.76	.51	-5.10	-1.21	6.78	20.20	-.87	2.15	1.91	-5.58	-.23	-.88	-6.08	1.45
9.05	-1.20	-2.0	.5	<-8.0	27.6	7	0.0920	-13.9	26.6	8.81	-4.41	.93	-4.86	-1.61	7.29	20.07	-.66	2.63	1.90	-5.98	-.08	-.68	-6.57	1.76
10.05	-1.20	-2.0	.5	<-8.0	26.2	7	0.0910	-13.9	26.6	10.17	-3.71	.51	-4.53	-1.65	7.23	19.59	-1.10	2.05	1.83	-8.97	.27	-1.00	-6.21	1.57
11.05	-1.20	-2.0	.5	<-8.0	26.9	8	0.0925	-14.3	28.9	10.03	-4.48	.91	-4.50	-1.90	7.23	21.14	-.22	2.79	1.42	-10.16	1.04	-1.17	-6.45	1.77
13.05	-1.40	-2.0	.5	<-8.0	26.9	8	0.0950	-14.3	28.8	9.62	-6.02	1.43	-4.28	-1.90	7.08	20.14	-.76	4.17	1.84	-11.70	.07	-.97	-6.73	1.74
14.05	-1.40	-2.0	.5	<-8.0	27.9	7	0.0900	-14.6	29.3	10.96	-5.89	1.17	-3.69	-2.32	7.68	21.18	-.11	3.78	2.19	-12.85	.02	-1.04	-6.81	1.77
5.05	-1.80	0	.5	-6.7	29.1	5	0.0920	-14.6	29.2	11.47	-6.08	1.45	-3.61	-2.28	7.10	20.42	-.71	4.44	1.32	-12.50	.69	-1.24	-7.58	1.94
6.05	-1.80	0	.5	-6.7	18.9	6	0.0870	-7.5	23.2	6.55	-1.76	.18	-3.57	-.86	6.80	14.68	-.47	.42	1.11	-.74	.63	-.55	-4.04	1.69
7.05	-1.10	0	.5	-6.7	20.5	5	0.0840	-8.2	24.0	7.54	-2.08	.33	-3.51	-.72	6.63	15.23	-.97	.93	.79	-1.27	.95	-.83	-4.22	1.83
8.05	-1.40	0	.5	-6.7	24.5	6	0.0875	-11.3	24.5	8.40	-2.63	.40	-3.05	-1.32	6.95	16.97	-.19	1.68	1.90	-3.72	.67	-.83	-5.00	1.23
9.05	-1.55	0	.5	-7.1	25.5	6	0.0895	-12.1	26.7	9.46	-3.97	.35	-3.14	-1.32	7.55	18.24	-.25	2.10	1.81	-5.78	.98	-.98	-5.19	1.09
10.05	-1.90	0	.5	-7.0	25.2	7	0.0900	-12.1	26.8	10.10	-4.74	.67	-2.91	-1.48	7.12	18.53	-.65	1.46	1.58	-7.14	1.07	-1.05	-5.67	1.14
4.05	-1.80	2.0	.5	-4.5	15.9	5	0.0840	-5.6	16.2	6.09	-1.26	.02	-2.17	-.33	5.23	11.06	-.07	1.04	.82	1.47	.73	-.26	-2.58	.46
5.05	-1.00	2.0	.5	-4.7	16.4	6	0.0865	-6.2	17.5	6.84	-1.76	.04	-1.85	-.62	5.74	11.85	.01	1.84	1.06	-.94	.88	-.36	-2.88	.66
6.05	-1.15	2.0	.5	-5.2	17.7	6	0.0890	-6.4	19.2	7.95	-2.38	.06	-1.86	-.75	6.40	12.86	-.14	1.40	1.05	-.82	1.31	-.61	-3.20	.77
8.05	-1.60	2.0	---	---	---	8	0.0950	-7.0	22.4	8.78	-3.24	.35	-1.22	-1.14	7.23	14.60	-.67	2.40	.85	-4.78	1.71	-.77	-4.53	.86
10.05	-2.00	2.0	---	---	---	6	0.0900	-9.0	25.9	10.10	-4.32	.66	-1.08	-1.50	6.98	15.60	-.17	2.93	1.39	-7.49	1.90	-.77	-5.06	.86
12.05	-2.20	2.0	.5	-8.0	24.5	6	0.0890	-10.0	24.5	10.34	-6.66	.66	-.55	-1.96	7.61	16.56	-.25	3.10	1.41	-10.04	.93	-1.00	-5.85	1.18
14.05	-2.40	2.0	.5	-7.4	24.0	7	0.0860	-10.8	24.4	11.49	-7.65	.59	-.57	-1.97	7.16	17.50	-.02	4.32	2.15	-13.51	1.63	-1.33	-5.67	1.69
(d) $\alpha_B = 12^\circ; \Delta\bar{A}_{0,s} = 3^\circ$																								
8.05	-1.00	4.0	2.7	-----	-----	4	0.0880	-12.6	26.6	11.54	-3.16	0.02	-2.60	-1.97	7.85	20.44	-0.10	1.67	1.52	-4.10	0.99	-0.82	-6.87	1.74
9.05	-1.10	4.0	3.5	-----	-----	4	0.0890	-12.6	26.7	12.18	-3.68	.05	-2.21	-2.03	8.77	20.51	1.22	3.57	1.19	-5.77	1.33	-.76	-7.22	1.70
6.05	-1.50	3.0	1.1	-----	-----	5	0.0885	-12.1	26.1	8.84	-1.93	.20	-2.13	-1.12	7.48	19.45	-.37	1.47	1.34	-1.99	.76	-1.02	-6.23	1.19
8.05	-1.50	3.0	2.0	-----	-----	5	0.0845	-12.6	26.6	10.01	-3.46	.65	-1.50	-1.73	6.19	19.46	-.17	1.85	.90	-4.18	.67	-1.02	-6.44	1.51
9.05	-1.55	3.0	2.5	-----	-----	5	0.0840	-12.6	29.5	10.96	-3.15	.42	-1.24	-1.60	7.73	20.11	-.68	2.22	.86	-6.11	.32	-.63	-7.80	.95
10.05	-1.45	3.0	3.1	-----	-----	4	0.0890	-12.6	29.1	11.26	-4.02	.58	-.82	-2.16	8.09	19.69	-.50	2.48	1.47	-8.57	.64	-1.00	-7.12	1.67
8.05	-1.00	2.0	2.5	-----	-----	4	0.0870	-11.0	25.4	11.26	-2.94	.23	-.66	-1.61	7.67	18.01	.31	2.48	1.61	-3.51	1.49	-.75	-5.69	1.24
9.05	-1.40	2.0	2.8	-----	-----	4	0.0845	-11.0	26.7	12.05	-3.82	.38	-.63	-1.73	7.25	18.61	-.34	1.99	.99	-5.20	1.73	-.82	-6.20	1.59
10.05	-1.45	2.0	2.5	-----	-----	4	0.0865	-11.6	26.8	12.56	-4.32	.41	-.47	-1.90	8.26	18.62	.31	3.90	1.29	-6.39	1.89	-1.01	-6.50	

TABLE VII. - ROTOR-BLADE MOTIONS AFTER RETURN OF CONTROL FROM A DISPLACEMENT TO THE ORIGINAL POSITION; NO FUSELAGE

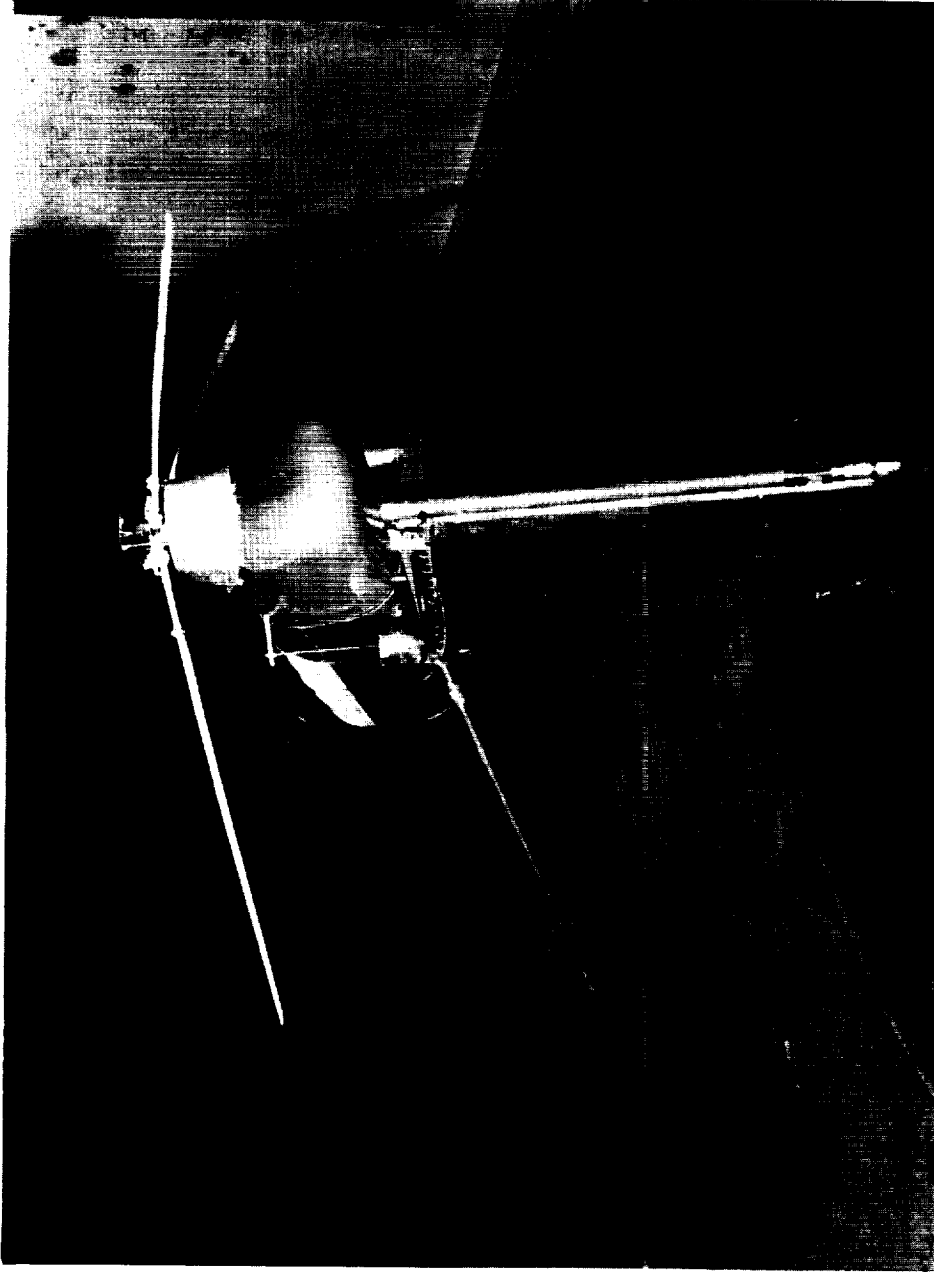
Nominal control, deg			Sec/rev	Feathering motion, deg					Flapping motion, deg					In-plane motion, deg				
$\bar{A}_{0,s}$	$\bar{A}_{1,s}$	$\bar{B}_{1,s}$		$A_{0,s}$	$A_{1,s}$	$A_{2,s}$	$B_{1,s}$	$B_{2,s}$	$a_{0,s}$	$a_{1,s}$	$a_{2,s}$	$b_{1,s}$	$b_{2,s}$	$E_0$	$E_1$	$E_2$	$F_1$	$F_2$
(a) $\alpha_s = 0^\circ$ ; return from $\Delta\bar{A}_{0,s} = 4^\circ$																		
9.0°	0	4.0	0.0915	8.10	-0.53	0.02	3.69	-0.18	4.24	4.16	0.52	3.15	1.02	-4.72	0.78	-0.20	-1.54	0.08
10.0°	0	4.0	0.0890	8.76	-0.92	.00	3.73	-.44	4.80	5.13	.48	3.44	1.15	-7.93	1.74	-.18	-1.15	.28
11.0°	0	4.0	0.0890	9.19	-1.35	.14	3.99	-.27	5.19	4.85	.37	4.31	1.25	-7.67	1.07	-.30	-1.83	-.04
12.0°	0	4.0	0.0850	9.98	-1.63	.28	3.83	-.63	4.96	5.30	.03	4.51	1.35	-7.93	1.49	-.50	-2.16	.17
13.0°	0	4.0	0.0855	10.31	-1.69	.06	4.09	-.66	5.38	6.05	.25	4.30	1.65	-10.44	1.96	-.59	-2.12	.41
14.0°	0	4.0	0.0855	11.36	-1.76	.37	4.15	-.88	5.48	6.28	-.06	5.00	1.55	-10.27	1.56	-.60	-2.68	.17
15.0°	0	4.0	0.0820	12.06	-2.16	.57	4.05	-.66	6.09	7.22	-.32	5.21	1.37	-11.95	1.33	-.75	-2.76	.05
(b) $\alpha_s = 0^\circ$ ; return from $\Delta\bar{A}_{0,s} = 4^\circ$																		
9.0°	-1.00	-4.0	0.0910	6.41	-3.18	0.65	-2.99	-1.06	6.55	15.32	-0.90	1.98	1.31	-3.27	2.00	-0.96	-4.22	1.44
9.0°	-1.10	-4.0	0.0920	7.35	-3.99	.36	-2.65	-1.29	7.11	14.91	-.84	1.92	1.88	-5.14	1.38	-.81	-4.78	1.03
10.0°	-1.15	-4.0	0.0910	7.07	-4.50	.85	-3.06	-1.25	7.14	15.19	-1.19	3.18	.90	-5.86	2.87	-1.04	-4.49	1.45
11.0°	-1.15	-4.0	0.0940	6.83	-5.85	1.02	-3.27	-1.37	7.59	14.18	-.13	5.36	2.45	-9.20	1.98	-.84	-5.25	1.19
9.0°	-1.65	0	0.0940	7.06	-3.08	.38	.07	-.77	6.11	10.81	.00	2.18	1.25	-5.45	1.40	-.51	-2.73	.37
10.0°	-1.68	0	0.0820	9.02	-2.85	.09	-.01	-.73	6.48	10.77	-.03	2.01	1.64	-6.73	1.98	-.70	-3.27	.76
12.0°	-2.35	0	0.0900	9.32	-4.82	.47	.51	-1.16	7.13	12.23	-.83	2.52	1.21	-12.21	2.55	-.81	-2.66	.72
8.0°	-1.65	2.0	0.0980	6.32	-3.50	.07	2.25	-.52	5.73	8.34	.33	2.46	1.18	-4.89	1.73	-.40	-2.51	.46
10.0°	-1.05	2.0	0.0915	8.42	-3.73	.16	2.33	-.66	6.70	9.57	-.01	2.42	1.09	-8.47	1.75	-.40	-2.60	.24
12.0°	-0.30	2.0	0.0840	9.46	-4.43	.30	3.07	-.96	6.48	8.89	-.28	2.36	1.55	-8.33	2.22	-.65	-3.21	.57
14.0°	-2.70	2.0	0.0845	9.71	-6.10	.75	3.05	-.88	6.51	9.43	-.48	3.54	1.52	-11.18	2.04	-.78	-4.21	.31
(c) $\alpha_s = 0^\circ$ ; return from $\Delta\bar{A}_{0,s} = 2^\circ$ ; $\Delta\bar{E}_{1,s} = 4^\circ$																		
9.0°	-0.80	-2.0	0.0945	4.89	-1.20	-0.05	-1.87	-0.51	5.88	10.87	0.76	1.27	1.14	0.15	0.40	-0.20	-2.40	0.53
9.0°	-0.85	-2.0	0.0900	5.47	-1.68	.09	-1.77	-.41	5.73	10.84	.10	1.29	.90	-.08	.02	-.09	-2.54	.18
9.0°	-1.05	-2.0	0.0905	6.92	-2.95	.21	-1.74	-.69	6.22	11.65	.08	2.61	1.12	-1.38	1.94	-.75	-2.77	.89
9.0°	-1.15	-2.0	0.0910	6.90	-2.85	.30	-1.80	-.86	6.11	11.70	.11	2.65	1.38	-3.04	1.75	-.54	-3.05	.67
9.0°	-1.10	-2.0	0.0925	7.41	-3.27	.30	-1.69	-1.02	6.87	12.70	-.15	2.98	1.16	-6.40	.78	-.39	-3.75	.56
10.0°	-1.10	-2.0	0.0920	7.23	-4.53	.51	-1.48	-1.15	6.40	12.12	-.35	3.62	1.76	-7.30	1.62	-.55	-4.02	.83
11.0°	-1.10	-2.0	0.0900	8.47	-4.31	.62	-1.74	-1.14	6.66	13.27	-.80	4.39	1.06	-8.38	2.42	-.78	-3.89	1.01
12.0°	-1.25	-2.0	0.0835	9.56	-4.16	.71	-1.59	-1.09	6.97	13.37	-.80	3.73	.88	-10.30	1.47	-.81	-3.75	.54
14.0°	-1.30	-2.0	0.0870	9.68	-5.01	.65	-1.71	-1.31	7.58	13.66	-.82	4.59	1.14	-11.85	2.05	-.97	-4.13	.67
9.0°	-1.35	-2.0	0.0875	9.27	-4.88	1.46	-.90	-1.41	6.91	12.86	-1.50	4.10	1.39	-11.98	1.52	-.86	-4.78	.83
9.0°	-1.80	0	0.0895	4.78	-1.18	-.04	.00	-.38	5.22	8.26	.54	1.37	.67	1.19	.08	.06	-2.11	.02
6.0°	-1.10	0	0.0895	5.36	-1.97	.12	.09	-.58	5.37	8.27	.10	1.71	.93	.49	1.17	-.32	-1.93	.41
8.0°	-1.10	0	0.0895	7.05	-2.64	.04	.36	-.59	6.21	9.37	.09	1.71	1.11	-4.82	1.22	-.41	-2.51	.31
9.0°	-1.15	0	0.0905	7.48	-3.98	.07	.82	-.73	6.62	10.00	.18	1.65	1.12	-5.20	.46	-.22	-3.18	.35
10.0°	-1.10	0	0.0895	8.06	-3.88	.07	.96	-.85	6.88	10.27	-.09	1.89	1.28	-6.08	.86	-.54	-3.26	.25
9.0°	-1.80	2.0	0.0880	4.16	-1.89	-.05	1.64	-.15	3.62	4.09	.31	.83	.75	1.74	-.09	.05	-.97	-.18
9.0°	-1.80	2.0	0.0890	4.81	-1.52	-.04	1.92	-.12	4.09	4.96	.59	1.25	.73	1.53	.48	-.05	-1.22	.10
9.0°	-1.15	2.0	0.0940	5.88	-1.65	.03	1.94	-.23	4.96	6.47	.41	1.44	.86	-1.46	.32	-.10	-1.57	-.01
8.0°	-1.10	2.0	0.0895	6.93	-2.94	.11	2.07	-.16	5.79	7.88	.34	2.70	1.19	-3.45	1.48	-.34	-2.46	.27
6.0°	-1.00	2.0	0.0895	8.20	-3.57	.17	2.60	-.67	6.26	8.58	-.13	2.15	1.38	-7.64	1.13	-.40	-2.66	.13
12.0°	-0.15	2.0	0.0895	9.40	-4.23	.40	2.85	-.79	6.98	9.11	-.45	2.26	1.36	-9.39	.65	-.40	-3.30	.08
14.0°	-0.10	2.0	0.0895	10.05	-5.00	.55	2.80	-.79	7.17	9.33	-.52	3.33	1.42	-11.19	1.87	-.63	-3.71	.46
(d) $\alpha_s = 12^\circ$ ; return from $\Delta\bar{A}_{0,s} = 4^\circ$																		
9.0°	-1.00	-4.0	0.0920	7.01	-3.96	0.29	-2.85	-1.17	8.07	16.14	0.00	2.72	1.89	-2.95	2.82	-0.89	-4.62	1.74
9.0°	-1.10	-4.0	0.0940	5.18	-1.59	.14	-2.43	-.85	7.80	14.76	-.65	1.87	.50	-.64	.65	-.59	-5.00	.27
9.0°	-1.05	-4.0	0.0870	5.83	-2.80	.21	-2.34	-.88	7.37	14.78	-.48	2.13	1.29	-1.01	.97	-.68	-4.66	.72
9.0°	-1.10	-4.0	0.0890	6.48	-3.02	.23	-2.06	-1.27	7.92	15.28	-.34	2.04	1.18	-5.00	2.04	-.89	-4.36	1.11
10.0°	-1.15	-4.0	0.0940	7.22	-4.38	.31	-1.32	-1.65	8.32	15.18	-.39	2.81	1.51	-8.08	1.84	-.86	-5.52	.77
11.0°	-1.10	-4.0	0.0890	6.89	-5.69	.35	-1.96	-.41	8.25	14.68	-.99	4.38	.65	-8.03	2.84	-.58	-5.06	1.19
9.0°	-1.00	-2.0	0.0900	7.63	-2.95	.25	-1.41	-1.12	7.53	14.29	.02	2.69	1.71	-.10	2.79	-.51	-5.45	1.18
9.0°	-1.10	-2.0	0.0900	7.99	-3.72	.40	-1.34	-.32	7.78	14.63	-.32	3.25	1.89	-6.09	2.16	-.75	-4.19	1.02
10.0°	-1.15	-2.0	0.0880	8.66	-3.95	.45	-1.29	-1.59	8.25	14.75	-.43	3.54	1.98	-7.40	2.61	-.83	-4.21	.92
11.0°	-1.15	-2.0	0.0880	9.34	-4.48	.74	-1.28	-1.91	7.90	15.25	-.92	3.98	1.94	-10.08	2.89	-1.07	-4.17	.50
12.0°	-1.15	-2.0	0.0890	9.60	-4.84	.88	-.47	-1.67	8.10	14.27	-1.25	3.46	1.80	-9.38	2.99	-.90	-4.36	.98
9.0°	-1.10	0	0.0910	7.83	-3.98	.42	.29	-.93	6.88	11.99	-.40	3.18	1.87	-4.27	2.70	-.73	-3.18	.69
9.0°	-1.10	0	0.0920	8.41	-2.98	.47	.54	-1.08	7.66	12.70	-.45	3.16	1.48	-7.24	2.35	-.80	-3.40	.40
10.0°	-1.10	0	0.0900	8.26	-4.00	.17	1.34	-1.19	7.70	12.19	-.56	3.12	1.70	-5.38	.90	-.41	-4.68	.51
11.0°	-1.10	0	0.0890	9.64	-3.89	.89	.68	-1.11	8.06	12.88	-.53	3.22	1.38	-9.70	2.10	-.80	-3.59	.59
12.0°	-1.05	0	0.0910	9.71	-5.12	.99	.12	-1.19	6.10	12.86	-.92	3.42	1.11	-12.66	3.73	-1.01	-3.07	.53
8.0°	-0.95	6.0	0.0910	7.17	-2.91	.16	0.14	-.37	5.89	9.20	.40	1.93	1.58	-4.41	.73	-.51	-2.24	-.41
10.0°	-0.75	6.0	0.0900	8.89	-3.40	.12	0.61	-.13	6.75	9.67	.14	2.11	1.58	-6.75	.94	-.57	-2.77	-.22
11.0°	-0.75	6.0	0.0910	9.45	-4.97	.44	0.67	-.86	6.70	6.40	-.20	2.55	1.91	-10.11	3.28	-.61	-2.55	-.28
12.0°	-0.70	6.0	0.0895	10.05	-4.15	.53	0.68	-.13	5.85	6.51	-.30	2.68	1.53	-10.17	3.98	-.64	-2.41	.20
14.0°	-0.15	6.0	0.0845	11.93	-5.98	.86	0.93	-.70	7.09	6.96	-.88	3.06	1.53	-12.03	3.74	-.73	-2.15	-.15
15.0°	-0.10	6.0	0.0835	11.96	-6.32	.96	0.93	-.85	7.60	7.77	-1.04	3.20	1.41	-13.76	3.74	-.73	-2.39	.10



L-90671

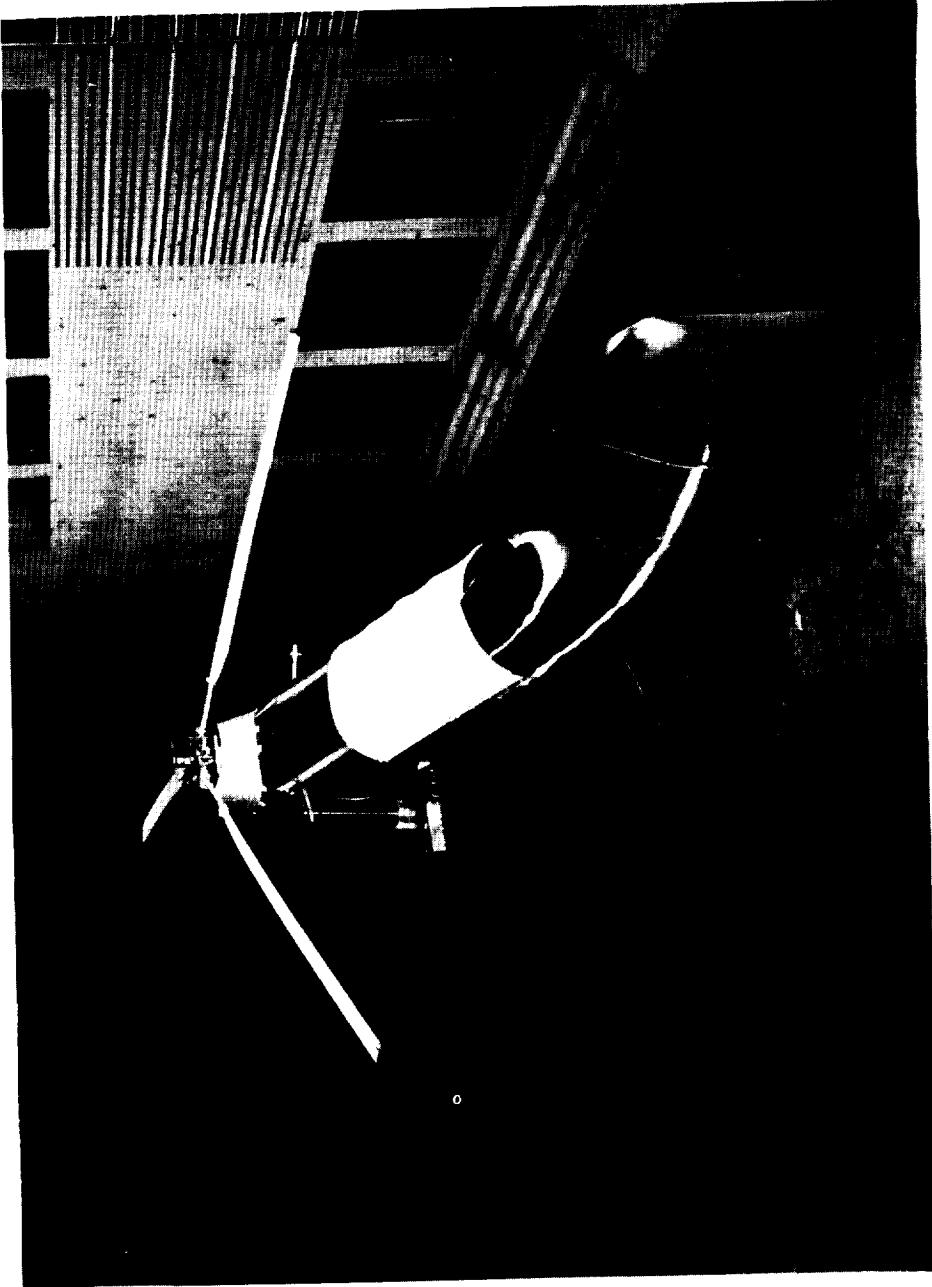
(a) Front view with fairing.

Figure 1.- Photographs of model.



(b) Front view with fuselage. L-90673

Figure 1.- Continued.



(c) Rear view with fuselage. L-90672

Figure 1.- Concluded.

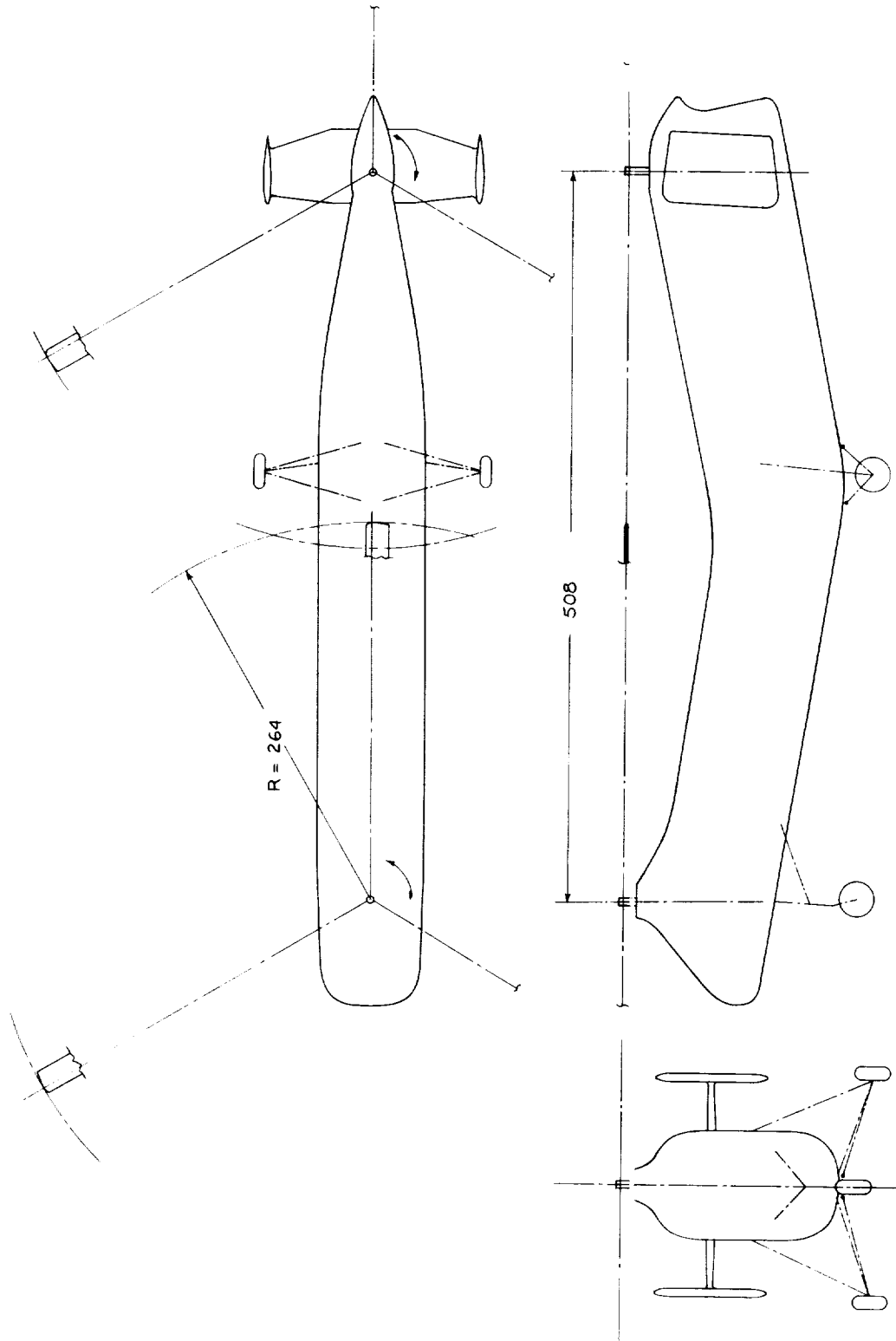


Figure 2.- General arrangement of the full-scale helicopter. (All dimensions are in inches.)

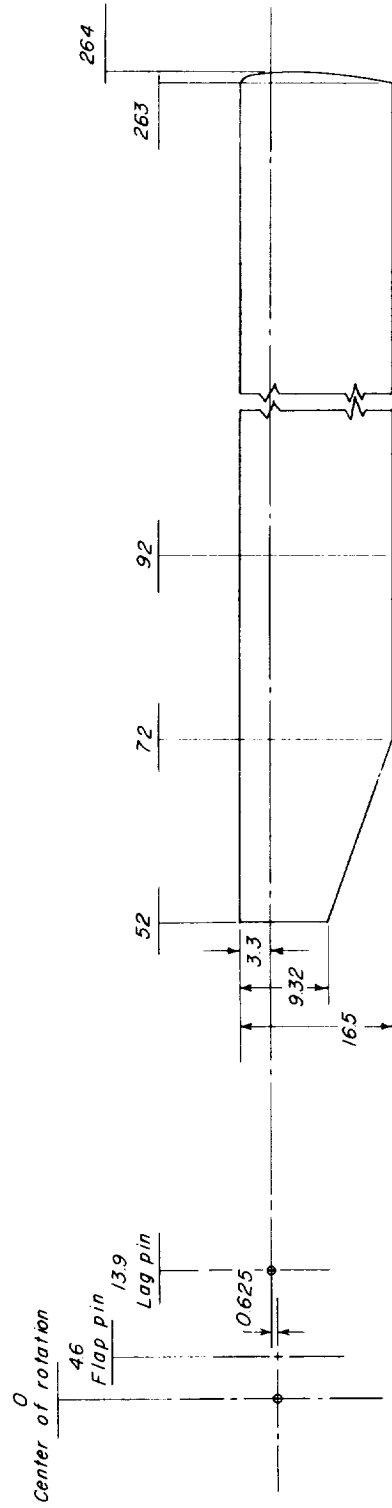


Figure 3.- Full-scale rotor blade. (All dimensions are in inches.)

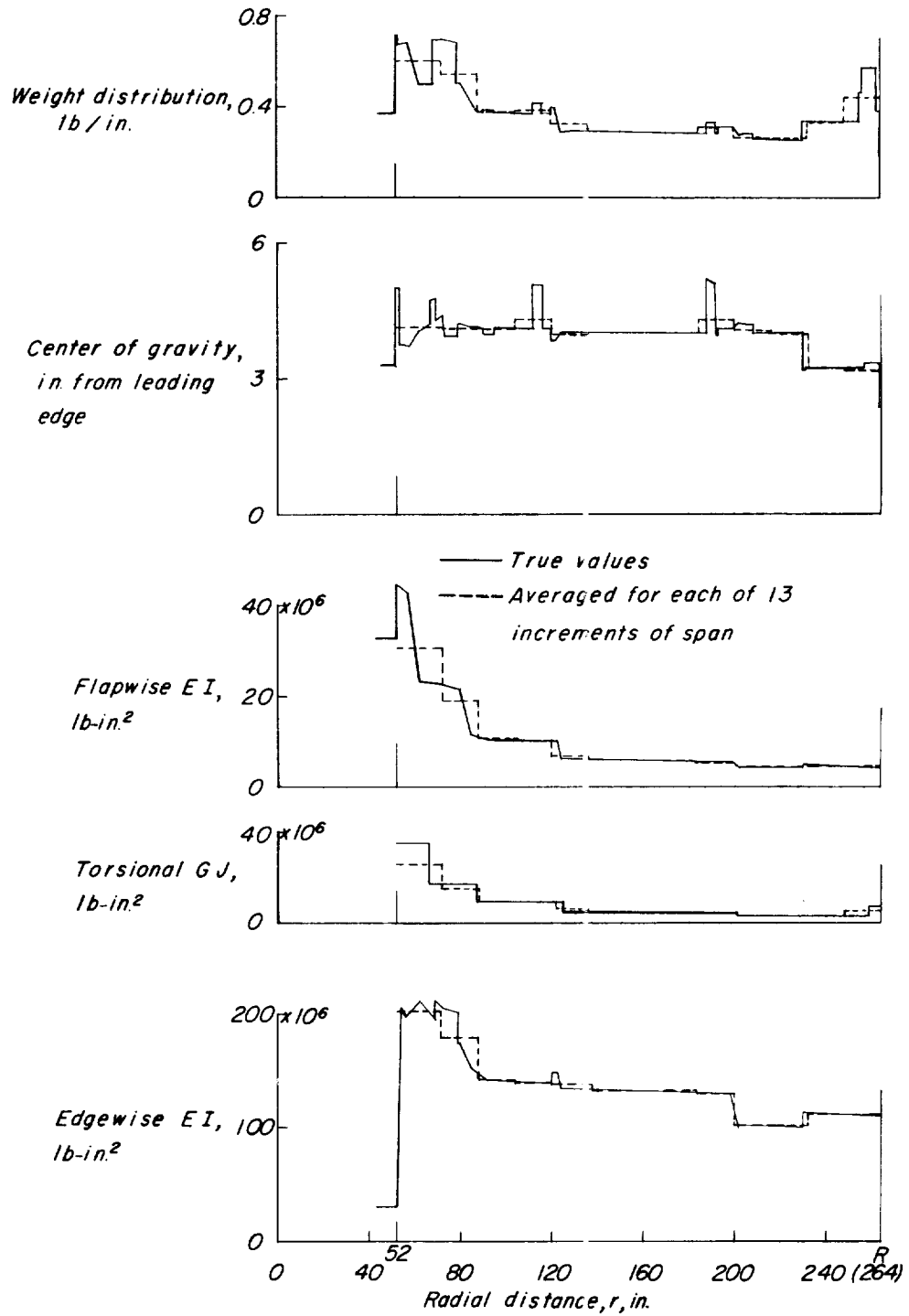
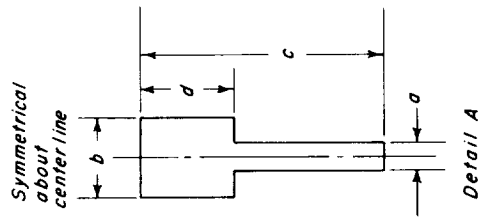
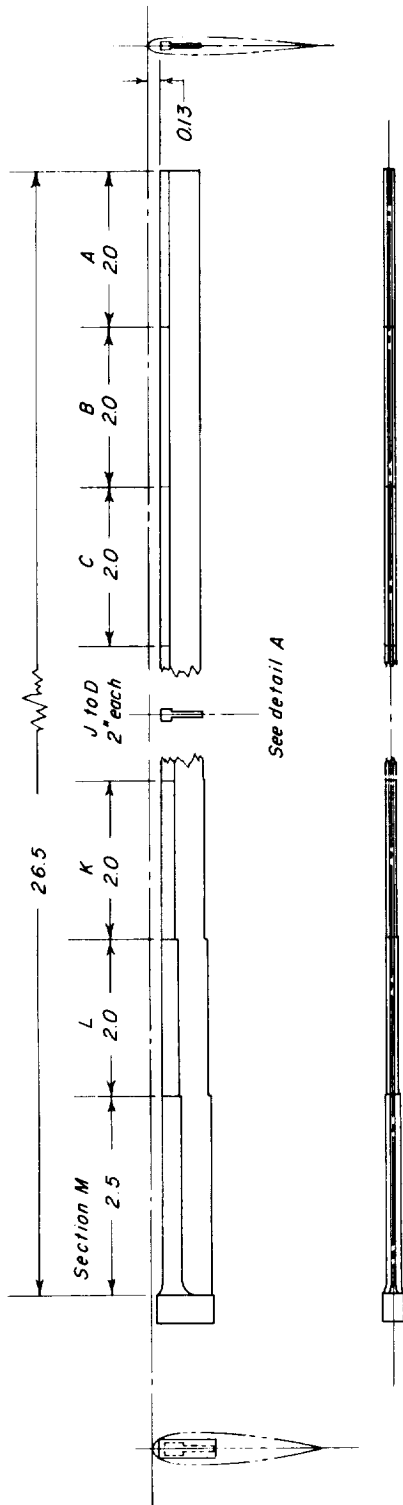
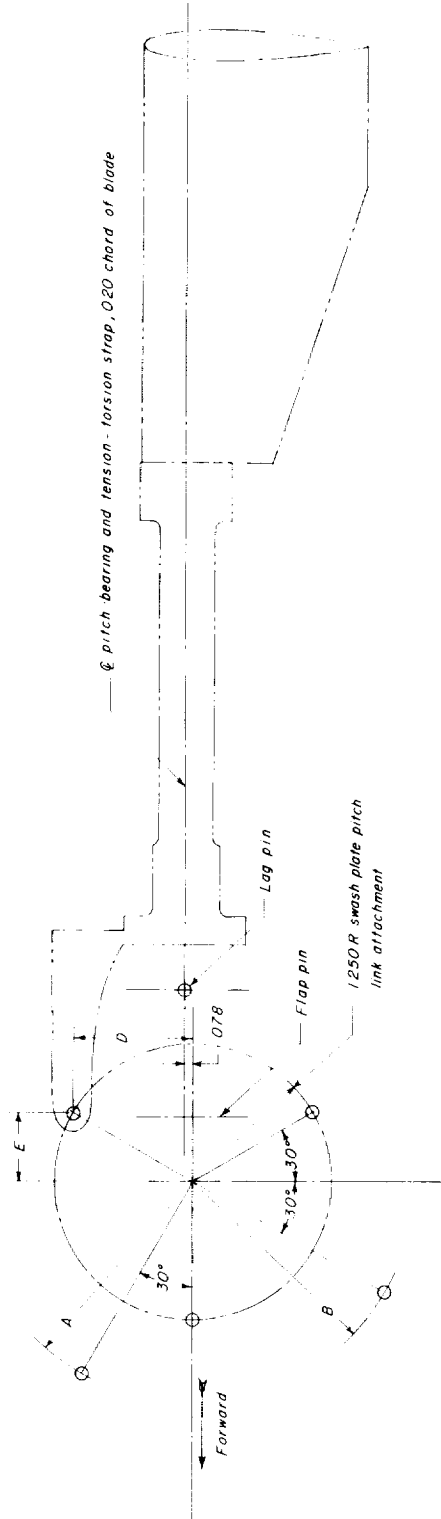


Figure 4.- Properties of full-scale rotor blades.



Section	a	b	c	d
A	0.030	0.1183	0.473	0.1259
B		.1190	.476	.1266
C		.1181	.461	.1257
D		.1195	.459	.1272
E		.1285	.498	.1366
F		.1296	.500	.1378
G		.1300	.503	.1383
H		.1305	.504	.1388
I		.1360	.507	.1447
J		.1454	.504	.1774
K		.1469	.507	.1792
L		.1689	.543	.2060
M	0.030	.1926	.558	.2349
Tolerance	±.0005	±.0005	±.001	±.001

Figure 5.- Details of spar construction of model blade. Material is hard rolled magnesium-alloy sheet. (All dimensions are in inches.)



Swash plate is shown in neutral position and blade with zero flap and lag angle and pitch at 075R of 8° 28'.  
 Longitudinal and lateral control link positions  
 A, radius (longitudinal), actual model = 2000, true scale = 1551  
 B, radius (lateral), actual model = 2000, true scale = 875  
 C, gap (lateral), actual model = .571, true scale = 400  
 Pitch links not vertical.  
 D, (upper end) = 1046, E = 0.635, F = 1500 (true length)

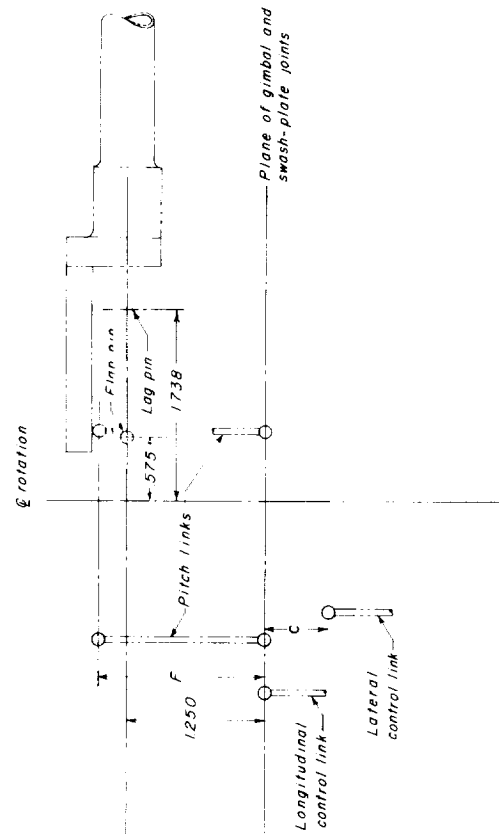


Figure 6.- Details of model rotor hub and swash plate. (All dimensions are in inches.)

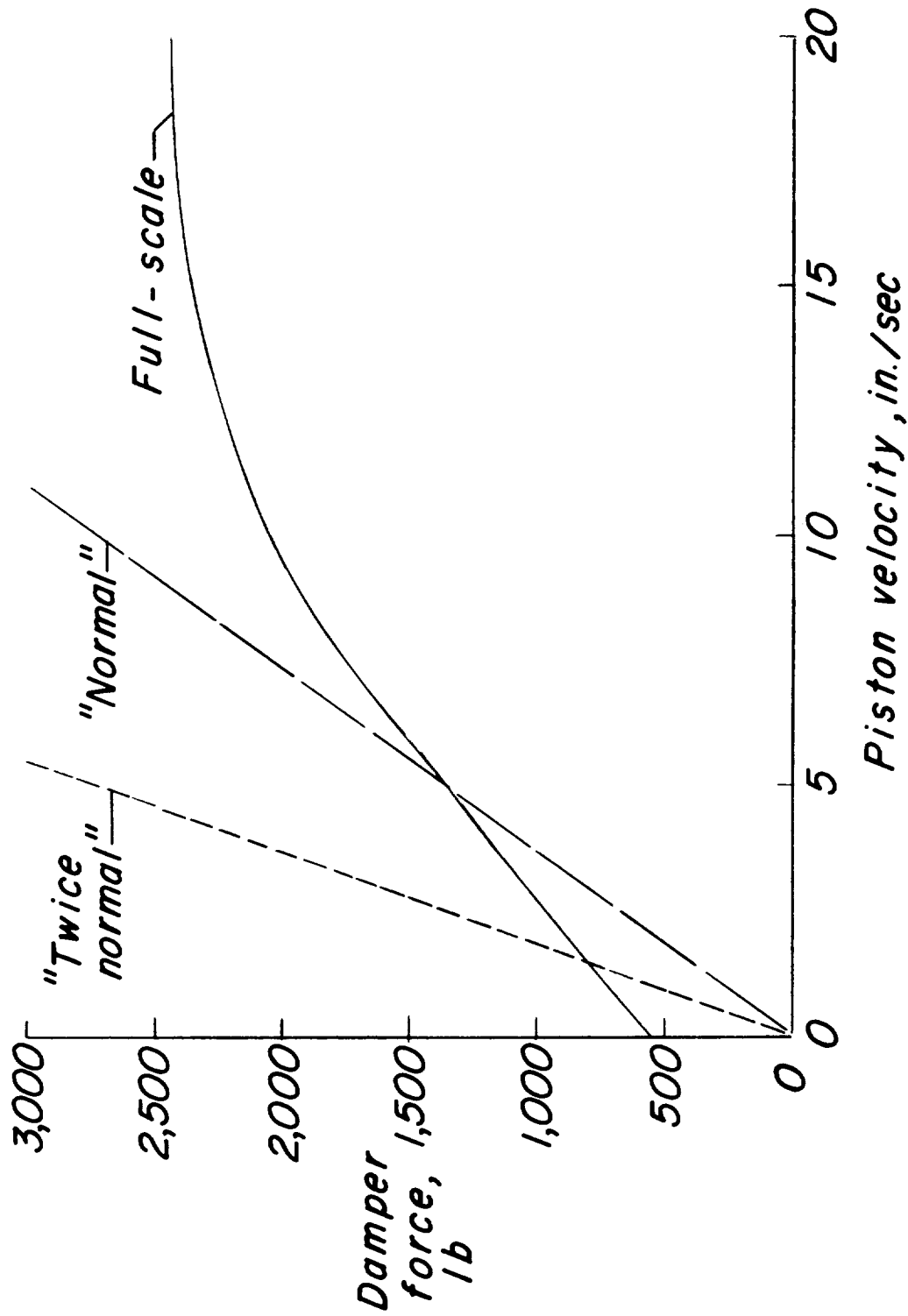


Figure 7.- Helicopter lag-damper characteristics and damping simulated by model dampers.

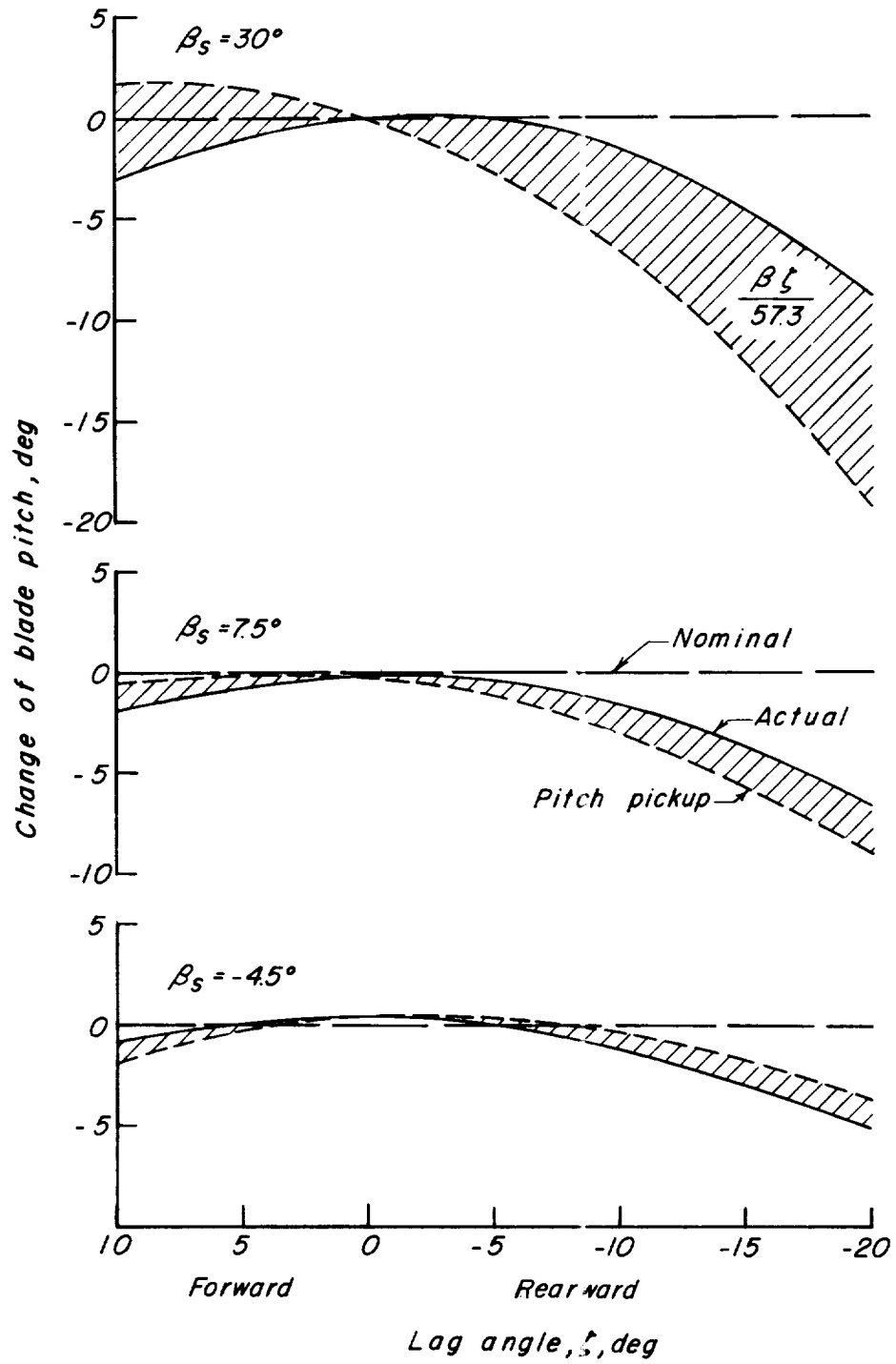


Figure 8.- Change of blade pitch angle with lag angle for a nominal pitch of  $8.5^\circ$  and three flapping angles.

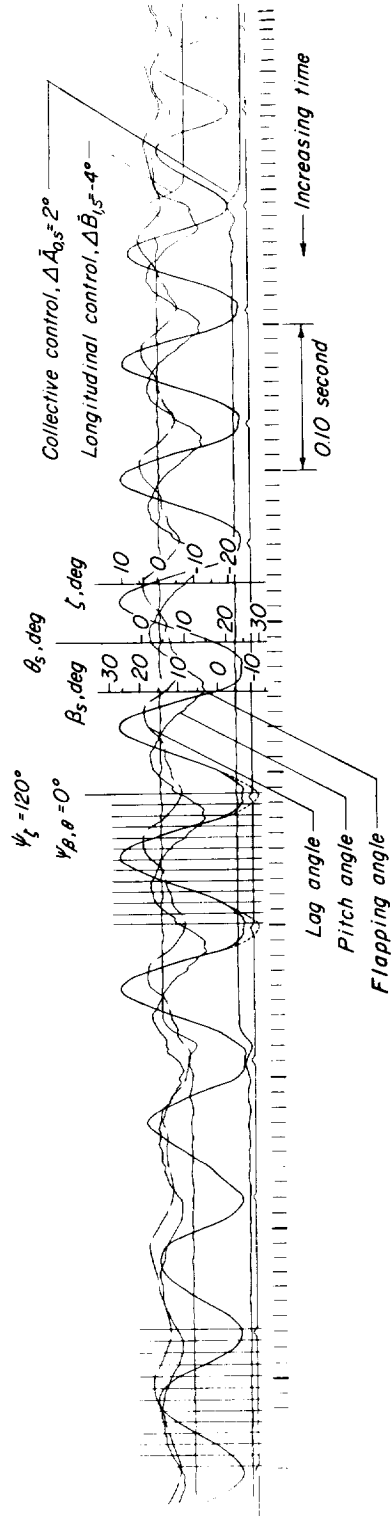


Figure 9.- Typical record of test.  $\alpha_s = 6^\circ$ ;  $\bar{A}_{0,s}(\text{initial}) = 6.05$ ;  $\bar{B}_{1,s}(\text{initial}) = -2$ . (Note that time increases from right to left.)

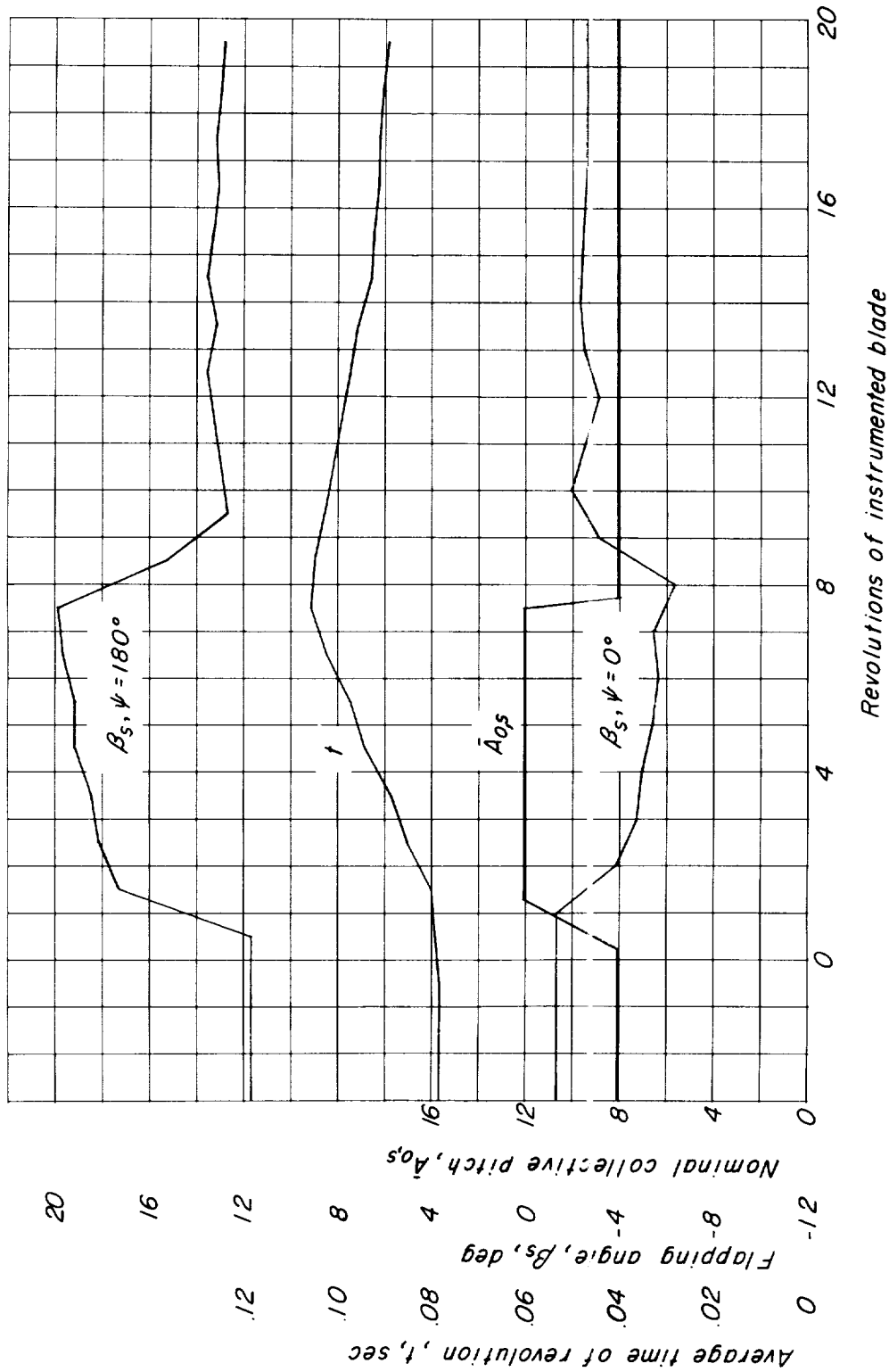


Figure 10.- Portion of time history.  $\alpha_s = 6^\circ$ ;  $\bar{A}_{0,s}$  (initial) = 8.05;  $\bar{B}_{1,s} = 2.0$ .